Table 1 Patient neurophysiology, serum anti-ganglioside characteristics and neuropathogenicity of the investigated sera

Serum number	Patient neurophysiology		Anti-ganglioside titer			GD3s-KO mouse tissue Pathophysiology			Wild-type mouse tissue Pathophysiology		
	CMAP	DML	GM1/GD1a complex	GM1	GD1a	fMEPP (/s)	Twitching	C3c staining	fMEPP (/s)	Twitching	C3c staining
Anti-GM1/GD1a-complex sera											
1	=	=	G-25600	G-800	G-6400	58.9	+	++	1.6	−	−
2	↓	=	G-12800	G-400	G-1600	49.3	++	+	3.2	−	−
3	↓	=	G-51200	G-400	G-800	45.0	++	+	NT	NT	NT
4	↓	=	G-12800	G-400	G-400	36.8	++	+++	0.5	−	NT
5	↓	⇑	G-6400	−	−	28.8	++	++	NT	NT	NT
6	=	=	G-6400	−	G-100	27.0	++	+++	0.6	−	NT
7	↓	=	G-12800	G-1600	G-100	19.8	++	+++	0.7	−	NT
8	↓	⇑	G-12800	G-1600	G-100	16.2	++	++	NT	NT	NT
9	↓	⇑	G-6400	G-100	G-100	14.2	++	++	NT	NT	NT
10	↓	=	G-6400	G-100	−	6.6	−	NT	1.7	−	+
11	↓	=	G-12800	−	G-200	4.9	+	NT	4.6	−	++
12	↓	⇑	G-400	M-200	−	3.5	−	NT	NT	NT	NT
13	=	⇑	G-6400	G-100	−	2.1	−	NT	0.5	−	NT
14	ND	ND	G-200	−	−	2.0	−	+	NT	NT	NT
15	↓	⇑	G-400	−	−	1.7	−	+	NT	NT	NT
16	↓	=	G-6400	−	−	1.6	−	NT	NT	NT	NT
17	=	=	G-400	−	−	1.4	+	NT	NT	NT	NT
18	=	=	G-3200	G-200	−	1.3	−	+	NT	NT	NT
19	↓	=	G-12800	G-100	G-800	1.1	−	NT	1.5	−	+++
20	↓	⇑	G-1600	G-200	G-100	1.1	−	NT	2.0	−	NT
21	↓	=	G-3200	G-800	G-400	1.1	−	−	NT	NT	NT
			GM1/GQ1b complex	GM1	GQ1b						
Anti-GM1/GQ1b-complex sera											
22	=	=	−†	−	−	1.6	−	+	7.2	−	+
23	=	=	G-1600	−	G-400	1.8	−	+	6.0	+	++
24	ND	ND	G-800	−	−	1.4	−	+	4.6	++	+
25	ND	ND	G-800	−	−	2.1	+	NT	4.3	+	NT
26	ND	ND	G-3200	−	G-400	1.5	−	NT	3.3	+	NT
27	=	=	G-1600	−	−	1.9	−	NT	2.3	+	NT
28	ND	ND	G-400	−	−	2.3	−	NT	2.3	−	NT
29	=	=	−†	M-100	−	1.3	+	NT	1.7	−	NT
30	↓	=	G-400	−	−	1.7	−	NT	1.6	+	NT
31	=	=	G-800	−	−	1.2	−	NT	1.6	+	NT

Patient neurophysiology, serum anti-ganglioside antibody activity (either IgG [G] or IgM [M]), effects on miniature end-plate potential (MEPP) frequency (fMEPP), muscle fiber twitching and C3c deposition at neuromuscular junctions of sera positive for either anti-GM1/GD1a antibodies (sera 1–21) or anti-GM1/GQ1b antibodies (sera 22–31). The sera have been ranked in descending order according to the observed MEPP frequency (for anti-GM1/GD1a-complex sera in GD3-synthase knockout [GD3s-KO] tissue and for anti-GM1/GQ1b-complex sera in wild-type tissue). Anti-ganglioside titer: −, negative; twitching: −, <1.0; +, between 1.0 and 2.0; ++, >2.0. C3c staining was carried out in two comparable runs on 17 and seven tissue samples. Shown is the relative intensity within these series: +, low; ++, moderate; +++, high. CMAP, compound muscle action potential; DML, distal motor latency; ND; no data available; NT, not tested.
†These sera were tested positive for anti-GM1/GQ1b-complex in the center of origin.

Pathophysiological effects at mouse NMJs

The antigenic ganglioside density on neuronal membranes is an important factor in the pathogenicity of anti-ganglioside 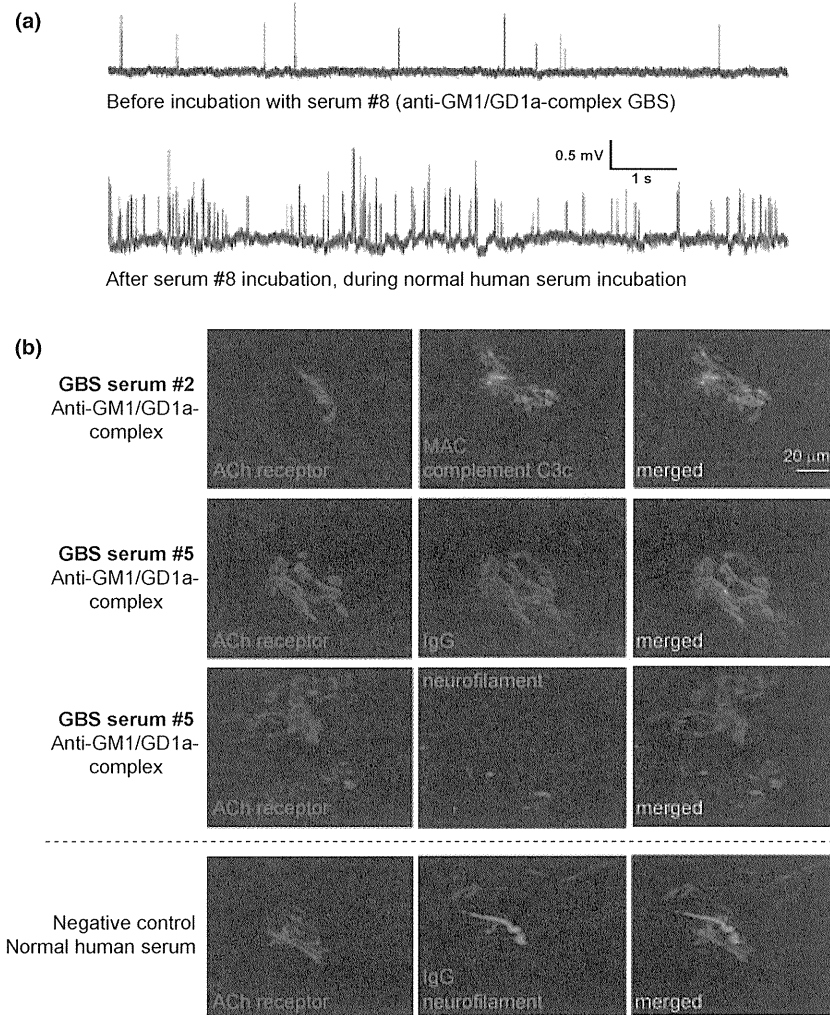antibodies.[12] To optimize our experimental model for anti-GM1/GD1a-complex antibodies, we used diaphragm muscles of GD3s-KO mice.[16] These mice genetically lack GD3-synthase and are therefore unable to synthesize b- and c-series gangliosides (Fig. 1). There is direct biochemical

− 35 −

proof that these mice upregulate the membrane density of a-series gangliosides GM1 and GD1a in the brain,[16] and we have previously shown indirectly with electrophysiological and fluorescence microscopical methods using anti-GD1a and anti-GM1 mAb that this is also the case at the motor nerve terminal membrane at the NMJ.[11,12] At GD3s-KO NMJs, 12 of the 21 anti-GM1/GD1a-complex sera induced elevations of MEPP frequency (i.e. >2.4/s, twice the control mean) during the NHS incubation (range 3.5–58.9/s; pooled control mean before incubations was 1.2/s; Figs 2a and 3a, Table 1). The elevated MEPP frequencies correlated positively and in a statistically highly significant way with the titer of the anti-GM1/GD1a-complex antibodies ($P < 0.01$, $r = 0.65$, Spearman's rank correlation test; Fig. 4). Such a positive correlation was not observed between elevated MEPP frequency and the titer of possible additionally present antibodies against single gangliosides GM1 ($P = 0.196$, $r = 0.30$) or GD1a ($P = 0.07$, $r = 0.4$). From 10 of the 21 sera, sufficient serum was available to be also studied at wild-type NMJs; only two of those sera (two and 11) induced (moderate) elevation of MEPP frequency (to 4.6 and 3.2/s, respectively; Table 1). With five of the 10 anti-GM1/GQ1b-complex sera, moderately elevated MEPP frequencies were observed (range 3.3–7.2/s) at wild-type NMJs, without correlation with anti-GM1/GQ1b-complex titer ($P = 0.74$, $r = 0.12$, Spearman's rank correlation test). No effect of these sera was observed on MEPP frequency at GD3s-KO NMJs (Fig. 2a, Table 1), which was as expected because the neuronal membranes of these mutant mice lack ganglioside GQ1b (Fig. 1).

The elevated MEPP frequency induced by anti-ganglioside-complex sera was generally accompanied by irregular twitching of individual muscle fibers throughout the preparation, (Fig. 2b, Table 1). Such twitches are most likely caused by superimposed MEPPs crossing the firing threshold of muscle fibers and have also been observed in our previous studies on the pathophysiological effects of sera positive for antibodies against single gangliosides and of mouse monoclonal antibodies against single gangliosides.[17,19] Mean twitching score was <0.5 in control (pre-incubation) sessions and was similarly low with anti-GM1/GD1a-complex sera tested in wildtype muscle (range 0.0–0.6). In GD3s-KO muscles, 11 of these 21 sera scored >1.0 (range 1.0–2.8; Fig. 2 b). Seven of the 10 investigated anti-GM1/GQ1b-complex sera scored >1.0 in wild-type muscles (range 1.2–2.3, Fig. 2b). At GD3s-KO muscles, two of these sera scored >1.0 (1.7 and 1.9). Mean
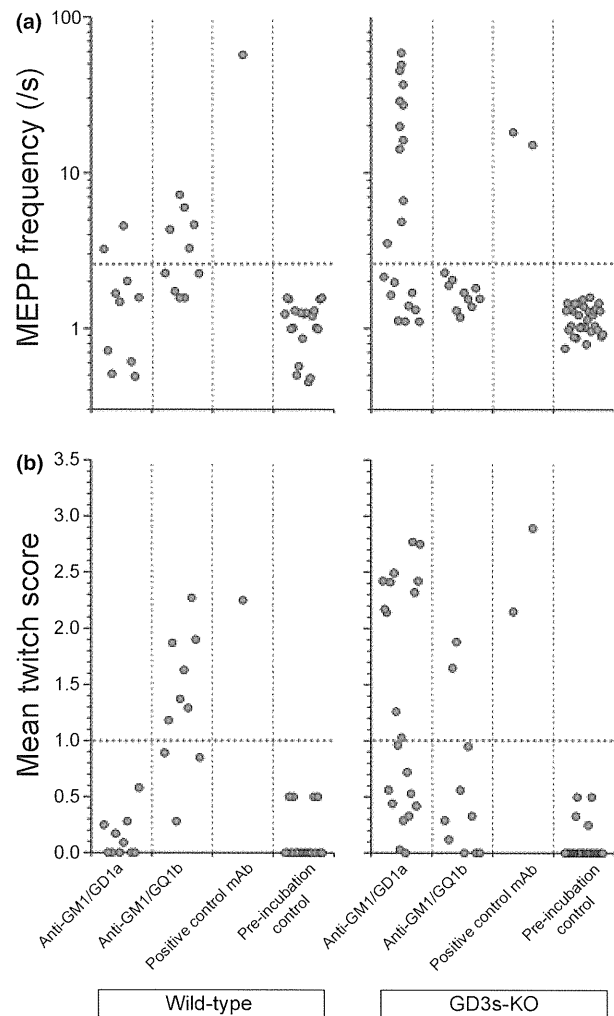
Figure 2 Overview of the neuropathophysiological effects of the investigated anti-ganglioside-complex sera. (a) Effect of anti-ganglioside-complex sera on of miniature end-plate potential (MEPP) frequency at wild-type (left panel) and GD3-synthase knockout (GD3s-KO; right panel) mouse diaphragm mouse neuromuscular junctions (NMJs). Twelve of the 21 tested anti-GM1/GD1a-complex sera induced MEPP frequency increases at GD3s-KO to a level of more than twice the pre-incubation control value (i.e. 2.4/s; dashed line). Just two of the 10 anti-GM1/GD1a-complex sera that could be tested at wild-type NMJs (modestly) increased MEPP frequency. Of the 10 investigated anti-GM1/GQ1b-complex sera, five induced (modest) MEPP frequency rise to levels of more than twice the control value, exclusively at wild-type NMJs. The anti-GQ1b mouse monoclonal antibodies (mAbs), CGM3, was used as a positive control in wild-type tissue; anti-GD1a mAb MOG35 and anti-GM1 mAb DG2 were used as positive controls in GD3s-KO tissue. (b) Effect of anti-ganglioside-complex sera on muscle fiber twitches at wild-type (left panel) and GD3s-KO (right panel) mouse NMJs. Most anti-ganglioside-complex sera that induced MEPP frequency elevation scored higher than 1 (dashed line) for muscle fiber twitching on visual inspection. Scoring: 0 = no twitching, 1 = twitching of <10 fibers, 2 = a small amount, 3 = a moderate amount and 4 = an extensive amount of fibers.

(a)

Before incubation with serum #8 (anti-GM1/GD1a-complex GBS)

0.5 mV

1 s

After serum #8 incubation, during normal human serum incubation

(b)

GBS serum #2
Anti-GM1/GD1a-
complex

GBS serum #5
Anti-GM1/GD1a-
complex

GBS serum #5
Anti-GM1/GD1a-
complex

Negative control
Normal human serum

Figure 3 Examples of electrophysiological and morphological effects of anti-ganglioside-complex sera on the mouse motor nerve terminal experimental model. (a) Examples of miniature end-plate potentials (MEPPs) recorded at GD3-synthase knockout (GD3s-KO) mouse diaphragm neuromuscular junctions (NMJs) before incubation with complement-inactivated anti-GM1/GD1a-complex serum 8 (upper trace) and during subsequent incubation of the serum pre-incubated muscle with normal human serum as the complement source (lower trace). Sweep length is 10 s. (b) Examples of C3c, membrane-attack complex (MAC), IgG and neurofilament immunostaining at diaphragm NMJs (delineated by fluorescently labeled α-bungarotoxin binding to acetylcholine receptors, left column panels). Muscle preparations had been exposed to complement-inactivated anti-GM1/GD1a-complex serum 2 (first row), serum 5 (second and third row) or complement-inactivated normal human serum (as negative control, fourth row), and were all subsequently exposed to normal human serum as the complement source. IgG and C3c deposition, and associated neurofilament loss are shown at anti-GM1/GD1a-complex sera-treated NMJs.

positive control mAb score was >2.1; that is, at GD3s-KO NMJs, the anti-GM1 mAb DG2 scored 2.9 and the anti-GD1a mAb MOG35 scored 2.2; whereas at wild-type NMJs, the anti-GQ1b mAb CGM3 scored 2.3.

Complement deposition at the NMJ

In our previous studies on antibodies against single gangliosides, we have shown that these can induce complement activation, culminating in membrane attack complex formation at the presynaptic nerve terminal and that this is underlying the observed temporary dramatic increase of MEPP frequency at the NMJ as a result of the excessive influx of Ca^{2+} through membrane attack complex pores in the pre-synaptic neuronal membrane.[17,20,21] We investigated here with confocal fluorescence microscopy whether anti-ganglioside-complex antibody-containing sera

also induced complement activation at the NMJ. For anti-GM1/GD1a-complex sera, complement C3c deposition at NMJs associated with elevated MEPP frequency ($P < 0.01$, Spearman's rank correlation test; Table 1, Fig. 3b). IgG and membrane attack complex deposition was observed at these NMJs, as well as neurofilament loss, indicating terminal motor axonal damage (Fig. 3b), as shown previously for antibodies against single gangliosides.[22] For anti-GM1/GQ1b-complex sera, C3c deposition at NMJs was sparse and not consistently associated with MEPP frequency elevation (Table 1).

Discussion

We report that sera positive for either anti-GM1/GD1a-complex or anti-GM1/GQ1b-complex antibodies clearly can produce pathophysiological effects at presynaptic neuronal membranes at NMJs
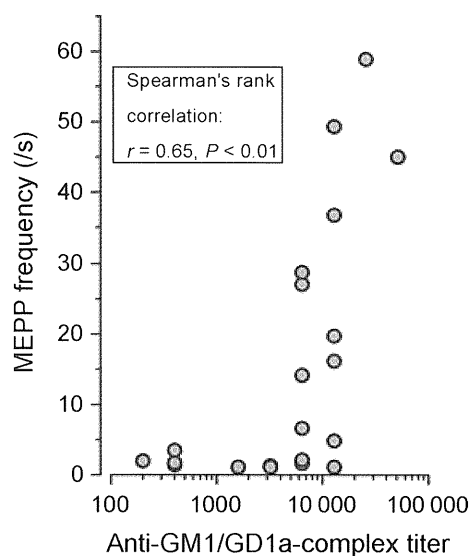
Figure 4 Positive correlation between anti-GM1/GD1a-complex titer of sera and the miniature end-plate potential (MEPP) frequency induced at mouse neuromuscular junctions (NMJs). Plot graph of the average MEPP frequency at NMJs of diaphragm muscles from GD3-synthase knockout mice induced by anti-GM1/GD1a-complex-positive GBS sera against the titer of the anti-GM1/GD1a-complex antibodies. Spearman's rank correlation test showed a highly significant positive correlation ($r = 0.65$, $P < 0.01$).

in the mouse diaphragm/phrenic nerve *ex vivo* experimental model. Roughly half of the 31 anti-ganglioside-complex sera tested in the current experiments induced the effects, which were similar to those observed earlier with antibodies and sera with activity against either single gangliosides GQ1b, GD1a, GM1 or GD1b.[4,11,12,21] In the set of 21 anti-GM1/GD1a-complex positive sera, we found a statistically highly significant correlation between the MEPP frequency elevation observed in the electrophysiological experiments and the titer of this specific anticomplex antibody in the sera and, furthermore, an association with complement activation as quantified in fluorescence microscopical analyses. In previous studies using sera or antibodies against single gangliosides, we showed that the utmost consequence at the mouse NMJ is a block of evoked ACh release as a result of presynaptic focal complement-mediated lysis, leading to muscle paralysis.[4] Although we did not structurally monitor in the present studies whether or not anti-ganglioside complex sera induced these end-point effects, some of them certainly caused a (partial) block of the diaphragm muscle contraction evoked by nerve stimulation, as judged visually. However, especially with the sera that only induced moderate increases in MEPP frequency, it is to be expected that they

would not, or only after periods much longer than the current observation period of 1 h, lead to transmission block.

Thus, we here for the first time show that anti-ganglioside-complex antibodies are capable of binding to living neuronal membranes and, by activating complement, can induce pathophysiological effects. These antibodies are therefore likely to be of pathogenic relevance, as also suggested by the clinical association with specific patterns of paralysis and, in some patient groups, mechanical ventilation.[2,8] In a previous study, anti-GM1/GD1a-complex serum positivity was associated with a pure motor variant of GBS without severe cranial nerve involvement,[9] suggesting a specific effect of these antibodies on motor axons. Our finding of deleterious effects of anti-ganglioside-complex antibodies at mouse motor nerve terminals suggests that these antibodies might, apart from causing motor axonal dysfunction, induce some degree of NMJ synaptopathy in GBS patients, potentially contributing to the paralytic symptoms.

As a result of the limited availability of most of the patient sera for repetitive experimental study and because of the heterogeneity of the anti-ganglioside(-complex) characteristics of the studied sera, some complexities of our results remain unresolved. First, not all sera induced the deleterious effects at mouse NMJs. Second, some of the active sera, especially those from the anti-GM1/GQ1b-complex positive series, caused only moderate effects; that is, the MEPP frequency remained lower than 10/s, as compared with values of >20 MEPP/s induced by the positive control mAbs and many of the active anti-GM1/GD1a-complex sera. These differences might relate to the titer and affinity variations of anti-ganglioside-complex antibodies amongst sera, together with the likely existence of an antibody binding threshold for the induction of pathophysiological effects at NMJs. Indeed, pathophysiological inactive or less active sera generally had low anti-ganglioside-complex titers and, at least in the anti-GM1/GD1a-complex series, statistical analysis showed a clear correlation between the elevated MEPP frequency and antibody titer. Third, many active sera, especially the anti-GM1/GD1a-complex positive sera, contained additional activities against single gangliosides GM1 and/or GD1a (Table 1), which in principle might have contributed to the effects. However, these single ganglioside antibody titers were generally (very) low, both in absolute sense, as well as relative to the titers of the anti-GM1/GD1a-complex antibody in these sera. Furthermore, there was no statistically significant correlation between the titer

of anti-GM1 or anti-GD1a antibodies and the elevated MEPP frequency observed with the sera. Still, this copresence of anti-single-ganglioside antibodies complicates interpretation, in particular, because four anti-GM1/GD1a-complex sera without additional activity against GM1 or GD1a lacked effects. This could be as a result of their only low-positive anti-GM1/GD1a-complex titers, but this might also suggest that besides anti-GM1/GD1a-complex activity, some additional anti-glycolipid or anti-glycolipid-complex activity is required for the neuropatho-physiological effects. Any potential copresence of anti-GQ1b single-ganglioside antibody in the anti-GM1/GD1a-complex sera active at GD3s-KO NMJs could not have been of influence, because GQ1b ganglioside is not expressed in the plasma membranes of GD3s-KO mice (Fig. 1). The strongest direct evidence for a neuropathophysiological effect of anti-GM1/GD1a-complex antibody came from the study of serum 5. The anti-GM1/GD1a-complex antibodies in this serum unambiguously were solely responsible for the complement-mediated neuropathophysiological effects at GD3s-KO NMJs, because this serum contained no additional anti-GD1a or -GM1 single-ganglioside antibodies. Some activity against GD1b ganglioside and GD1b- and GQ1b-containing ganglioside complexes was detected in this serum (data not shown), but this was irrelevant because GD3s-KO tissue lacks the b-series gangliosides GD1b and GQ1b (Fig. 1). Thus, the results obtained with this particular serum clearly provide proof-of-principle that GBS anti-ganglioside-complex antibodies can induce neuropathophysiological effects at living neuronal membranes.

Activity against the single gangliosides GM1 or GQ1b was less of a confounding factor in the GM1/GQ1b-complex group, where seven of the 10 sera lacked single ganglioside antibodies. However, just three of those induced MEPP frequency elevations at wild-type NMJs and these effects were only rather modest in magnitude. In addition, complement deposition and muscle fibre twitching did not correlate very well with elevation of MEPP frequency. No statistically significant correlation was found between the anti-GM1/GQ1b-complex antibody titer of the sera in this series and the MEPP frequency that was observed at wild-type NMJs. This shows that anti-GM1/GQ1b antibodies generally only induce relatively weak neuropathogenic effects in this experimental model.

Anti-GM1/GD1a-complex sera induced either no neuropathophysiological effects or much less intense effects at wild-type NMJs, as compared with GD3s-

KO NMJs. This shows the requirement of an elevated anti-GM1/GD1a-complex antigen density for anti-GM1/GD1a-complex antibodies to become neuropathogenic, because the a-series gangliosides GM1 and GD1a are upregulated in neuronal membranes of GD3s-KO mice, including motor nerve terminals.[12,16] The ganglioside and ganglioside-complex expression pattern in different peripheral nerve membrane domains might vary considerably, both within and between species. It is even possible that certain GBS patients express particular predisposing ganglioside-complex densities or configurations. Development of high-affinity mouse mAbs specific for ganglioside-complexes will be an essential next step, allowing more detailed experimental studies in which these issues can be explored.

Acknowledgements

References

1. Kaida K, Kusunoki S. Antibodies to gangliosides and ganglioside complexes in Guillain–Barre syndrome and Fisher syndrome: mini-review. *J Neuroimmunol.* 2010; **223**: 5–12.
2. Notturno F, Luciani M, Caporale CM, Ciarelli A, Uncini A. Antibodies to ganglioside complexes in Guillain–Barre syndrome: clinical correlates, fine specificity and complement activation. *Int J Immunopathol Pharmacol.* 2009; **22**: 437–45.
3. van Doorn PA, Ruts L, Jacobs BC. Clinical features, pathogenesis, and treatment of Guillain–Barre syndrome. *Lancet Neurol.* 2008; **7**: 939–50.

4. Plomp JJ, Willison HJ. Pathophysiological actions of neuropathy-related anti-ganglioside antibodies at the neuromuscular junction. *J Physiol.* 2009; **587**: 3979–99.

5. McGonigal R, Rowan EG, Greenshields KN, Halstead SK, Humphreys PD, Rother RP, et al. Anti-GD1a antibodies activate complement and calpain to injure distal motor nodes of Ranvier in mice. *Brain.* 2010; **133**: 1944–60.

6. Kaida K, Morita D, Kanzaki M, Kamakura K, Motoyoshi K, Hirakawa M, et al. Ganglioside complexes as new target antigens in Guillain–Barre syndrome. *Ann Neurol.* 2004; **56**: 567–71.

7. Kusunoki S, Kaida K, Ueda M. Antibodies against gangliosides and ganglioside complexes in Guillain–Barre syndrome: new aspects of research. *Biochim Biophys Acta.* 2008; **1780**: 441–4.

8. Kaida K, Morita D, Kanzaki M, Kamakura K, Motoyoshi K, Hirakawa M, et al. Anti-ganglioside complex antibodies associated with severe disability in GBS. *J Neuroimmunol.* 2007; **182**: 212–8.

9. Kuijf ML, Godschalk PC, Gilbert M, Endtz HP, Tio-Gillen AP, Ang CW, et al. Origin of ganglioside complex antibodies in Guillain–Barre syndrome. *J Neuroimmunol.* 2007; **188**: 69–73.

10. Kaida K, Kanzaki M, Morita D, Kamakura K, Motoyoshi K, Hirakawa M, et al. Anti-ganglioside complex antibodies in Miller Fisher syndrome. *J Neurol Neurosurg Psychiatry.* 2006; **77**: 1043–6.

11. Greenshields KN, Halstead SK, Zitman FM, Rinaldi S, Brennan KM, O'Leary C, et al. The neuropathic potential of anti-GM1 autoantibodies is regulated by the local glycolipid environment in mice. *J Clin Invest.* 2009; **119**: 595–610.

12. Goodfellow JA, Bowes T, Sheikh K, Odaka M, Halstead SK, Humphreys PD, et al. Overexpression of GD1a ganglioside sensitizes motor nerve terminals to anti-GD1a antibody-mediated injury in a model of acute motor axonal neuropathy. *J Neurosci.* 2005; **25**: 1620–8.

13. Goodyear CS, O'Hanlon GM, Plomp JJ, Wagner ER, Morrison I, Veitch J, et al. Monoclonal antibodies raised against Guillain–Barre syndrome-associated Campylobacter jejuni lipopolysaccharides react with neuronal gangliosides and paralyze muscle-nerve preparations. *J Clin Invest.* 1999; **104**: 697–708.

14. Kaida K, Kusunoki S, Kanzaki M, Kamakura K, Motoyoshi K, Kanazawa I. Anti-GQ1b antibody as a factor predictive of mechanical ventilation in Guillain–Barre syndrome. *Neurology.* 2004; **62**: 821–4.

15. Zitman FM, Todorov B, Jacobs BC, Verschuuren JJ, Furukawa K, Furukawa K, et al. Neuromuscular synaptic function in mice lacking major subsets of gangliosides. *Neuroscience.* 2008; **156**: 885–97.

16. Handa Y, Ozaki N, Honda T, Furukawa K, Tomita Y, Inoue M, et al. GD3 synthase gene knockout mice exhibit thermal hyperalgesia and mechanical allodynia but decreased response to formalin-induced prolonged noxious stimulation. *Pain.* 2005; **117**: 271–9.

17. O'Hanlon GM, Plomp JJ, Chakrabarti M, Morrison I, Wagner ER, Goodyear CS, et al. Anti-GQ1b ganglioside antibodies mediate complement-dependent destruction of the motor nerve terminal. *Brain.* 2001; **124**: 893–906.

18. Willison HJ, Veitch J, Swan AV, Baumann N, Comi G, Gregson NA, et al. Inter-laboratory validation of an ELISA for the determination of serum anti-ganglioside antibodies. *Eur J Neurol.* 1999; **6**: 71–7.

19. Jacobs BC, Bullens RW, O'Hanlon GM, Ang CW, Willison HJ, Plomp JJ. Detection and prevalence of alpha-latrotoxin-like effects of serum from patients with Guillain–Barre syndrome. *Muscle Nerve.* 2002; **25**: 549–58.

20. Halstead SK, O'Hanlon GM, Humphreys PD, Morrison DB, Morgan BP, Todd AJ, et al. Anti-disialoside antibodies kill perisynaptic Schwann cells and damage motor nerve terminals via membrane attack complex in a murine model of neuropathy. *Brain.* 2004; **127**: 2109–23.

21. Plomp JJ, Molenaar PC, O'Hanlon GM, Jacobs BC, Veitch J, Daha MR, et al. Miller Fisher anti-GQ1b antibodies: alpha-latrotoxin-like effects on motor end plates. *Ann Neurol.* 1999; **45**: 189–99.

22. O'Hanlon GM, Humphreys PD, Goldman RS, Halstead SK, Bullens RW, Plomp JJ, et al. Calpain inhibitors protect against axonal degeneration in a model of anti-ganglioside antibody-mediated motor nerve terminal injury. *Brain.* 2003; **126**: 2497–509.

23. Svennerholm L. Designation and schematic structure of gangliosides and allied glycosphingolipids. *Prog Brain Res.* 1994; **101**: XI–XIV.

MINI-REVIEW

Antibodies against ganglioside complexes in Guillain–Barré syndrome and related disorders

Susumu Kusunoki* and Ken-ichi Kaida†

*Department of Neurology, Kinki University School of Medicine, Osaka, Japan
†Third Department of Internal Medicine, National Defense Medical College, Saitama, Japan

Abstract

Guillain-Barré syndrome (GBS) is acute autoimmune neuropathy, often subsequent to an infection. Serum anti-ganglioside antibodies are frequently elevated in titer. Those antibodies are useful diagnostic markers and possible pathogenetic factors. Recent data demonstrated that sera from some patients with GBS react with ganglioside complexes (GSCs) consisting of two different gangliosides, but not with each constituent ganglioside. Those antibodies may specifically recognize a new conformational epitope formed by two gangliosides. In particular, the antibodies against GD1a/GD1b and/or GD1b/GT1b complexes are associated with severe GBS requiring artificial ventilation. The antibodies to GM1/GalNAc–GD1a and those to GSCs containing GQ1b or GT1a are associated with pure motor GBS and Fisher syndrome, respectively. In contrast, the binding activities of the antibodies highly specific to GD1b are strongly inhibited by the addition of GD1a to GD1b. Gangliosides along with other components as cholesterol are known to form lipid rafts, in which two different gangliosides may form a new conformational epitope. Future investigation is necessary to elucidate the roles of GSCs in the plasma membrane and of the clinical relevance of the anti-GSCs antibodies.

Keywords: ganglioside, Guillain-Barré syndrome, membrane microdomain, peripheral nerve.

J. Neurochem. (2011) 116, 828–832.

Anti-ganglioside antibodies, mostly IgG type, are present in the sera from approximately 60% of patients with Guillain-Barré syndrome (GBS), acute immune-mediated polyradiculoneuropathy (Willison and Yuki 2002; Kusunoki et al. 2008; Van Doorn et al. 2008). Because the presence of anti-ganglioside antibodies in the acute-phase sera is a characteristic feature of GBS, those antibodies can be used as diagnostic markers of GBS. There are many molecular species of gangliosides, named depending on the carbohydrate sequences. Each ganglioside has unique distribution within the PNS. Considering the gangliosides are localized in the plasma membrane with their carbohydrate portions extended to the extracellular spaces, the anti-ganglioside antibodies may function in the pathogenesis of GBS through antibody-antigen interaction in PNS.

IgG anti-GQ1b antibody is one of the best studied antibodies. Ig anti-GQ1b antibodies are specifically associated with a variant of GBS, Fisher syndrome (FS) characterized by ophthalmoplegia and ataxia (Chiba et al. 1992). Anti-GQ1b monoclonal antibody specifically immunostains paranodal myelin of human cranial nerves innervating extraocular muscles (Chiba et al. 1993) and some large neurons in dorsal root ganglia (Kusunoki et al. 1999). It has recently been reported that the neuromuscular junctions of human extraocular muscles are richly bound by the antibodies against GQ1b and GT1a (Liu et al. 2009). Thus, the anti-GQ1b antibodies may cause opthalmoplegia and ataxia by binding to the regions where GQ1b is densely localized.

Measurement of anti-ganglioside antibodies has been conducted with ELISA or TLC-immunostaining by the use of purified single ganglioside antigens. Gagliosides have characteristics of forming clusters in the plasma membrane

(Hakomori 2002). In the clusters, the carbohydrate structure of a ganglioside may interact with each other to form a novel epitope. We recently demonstrated that some GBS patients had serum antibodies that specifically recognize the novel glycoepitopes formed by two individual ganglioside molecules and named such antibodies as 'anti-ganglioside complex (GSC) antibodies' (Kaida et al. 2004).

Antibodies to ganglioside complexes in GBS

Antibodies to GD1a/GD1b and GD1b/GT1b complexes in severe GBS

Anti-GD1a/GD1b complex antibodies are the first identified antibodies against GSCs. We investigated a serum from a GBS patient who showed acute severe flaccid tetraparesis and needed artificial ventilation. We found an unidentified immuno-reactive band in the position just below GD1a on TLC of a crude ganglioside fraction from bovine brain. The serum was not reactive with any of such purified gangliosides as GM1, GM2, GM3, GD1a, GD1b, GD3, GalNAc–GD1a, GT1b, and GQ1b. But the serum IgG bound strongly to the well coated with the mixture of GD1a and GD1b gangliosides (GD1a/GD1b complex). When GD1a and GD1b were developed in the same lane on TLC using a developing solvent, chloroform/methanol/0.2%CaCl$_2$·2H$_2$O (50 : 45 : 10), the serum IgG strongly immunostained just the overlapping portion between GD1a and GD1b. When another developing solvent (C/M/0.2%CaCl$_2$·2H$_2$O, 30/65/10) that completely separated the positions of GD1a and GD1b was used, no immunoreaction was identified. Those data indicate that mixing GD1a and GD1b may produce a new conformational glycoepitope which is different from that of GD1a or GD1b alone and the antibody in sera from the above patient may specifically recognize such a new glycoepitope.

We next investigated antibodies in sera from 234 GBS patients with ELISA using a mixture of two of the four major gangliosides (GM1, GD1a, GD1b and GT1b) (Kaida et al. 2007). The sera with anti-GSC antibodies often exhibited to some extent reactivity with constituent gangliosides of the GSCs. When optical density for the anti-GD1a/GD1b antibody was 0.2 higher than that corresponding to anti-GD1a or anti-GD1b antibody or it was more than the sum of those of anti-GD1a and anti-GD1b antibodies, the sera were judged to be anti-GD1a/GD1b-positive. The same criteria also were applied to the other GSCs. The cutoff value (0.2) for anti-GSC antibodies was decided arbitrarily. The results showed that 39 of 234 patients (17%) had antibodies against at least one of the mixture antigens. All the 39 patients had anti-GM1/GD1a antibodies, 27 had anti-GM1/GT1b antibodies, 16 had anti-GD1a/GD1b antibodies, and 13 had GD1b/GT1b antibodies. Most of anti-GD1a/GD1b or anti-GD1b/GT1b antibody reacted also with GM1/GT1b as well

as GM1/GD1a. Immunoabsorption study suggested that anti-GSC antibodies specifically react with clustered glycoepitopes common to these GSCs, rather than individually with each GSC. An epitope formed by a combination of [Galβ1-3GalNAc] and [NeuAcα2-3Galβ1-3GalNAc] in the terminal moieties of ganglio-N-tetraose structures is likely to be essential for the antibody binding. Among them, antibodies against GD1a/GD1b and GD1b/GT1b complexes were significantly associated with severe GBS requiring artificial ventilation (Kaida et al. 2007). Those antibodies can be useful markers of severe GBS. Future study is needed to clarify why anti-GD1a/GD1b and GD1b/GT1b antibodies are associated with severe disabilities.

### Antibodies to ganglioside complexes including GQ1b

Because FS is considered to be a variant of GBS, we extended an investigation of anti-GSC antibodies to FS patients. Presence of anti-ganglioside complexes antibodies in FS therefore was investigated with ELISA using seven ganglioside antigens; GM1, GM2, GD1a, GD1b, GT1a, GT1b and GQ1b (Kaida et al. 2006).

Acute phase serum samples were collected from 12 FS patients, 10 of whom had IgG anti-GQ1b antibodies. ELISA results showed that seven patients had antibodies to GSCs such as GQ1b/GM1, GQ1b/GD1b, GQ1b/GD1a, GQ1b/GT1b, GT1a/GM1, GT1a/GD1b, and GT1a/GD1a, but not to the complexes without GQ1b and GT1a. One patient had no anti-GQ1b or anti-GT1a antibodies, but had antibodies to GQ1b/GM1 and GT1a/GM1. Specific immunoreactivities against the overlapping portion of the two gangliosides were confirmed by TLC-immunostaining. In contrast to GBS, no FS patients had antibodies to the complexes consisting of two of the four major gangliosides, GM1, GD1a, GD1b and GT1b.

The results of anti-GSCs antibody assay on larger number of patients with FS and those with GBS with opthalmoplegia indicated that the serum antibodies could be subdivided into the three groups (Kanzaki et al. 2008): (i) antibodies specific to GQ1b and/or GT1a without anti-GSCs reactivity; (ii) antibodies that recognize a combination of [Galβ1-3GalNAc] and [NeuAcα2-8 NeuAcα2-3Galβ1-3GalNAc] in the terminal residues of ganglio-N-tetraose structures, such as antibodies to GQ1b/GM1, GQ1b/GD1b, GT1a/GM1, GT1a/GD1b (Fig. 1); and (iii) antibodies that recognize a combination of [NeuAcα2-3Galβ1-3GalNAc] and [NeuAcα2-8 NeuAcα2-3Galβ1-3GalNAc] in the terminal residues, such as antibodies to GQ1b/GD1a, GT1a/GD1a, GQ1b/GT1b, GT1a /GT1b. In addition, recent report showed that some patients have the antibodies specific to GQ1b/GA1 (Ogawa et al. 2009).

Sensory signs were infrequent in FS patients with antibodies to GQ1b/GM1 but were frequent in patients with other types of antibodies. However, the clinical relevance of such anti-GSC antibodies needs to be investigated in future.
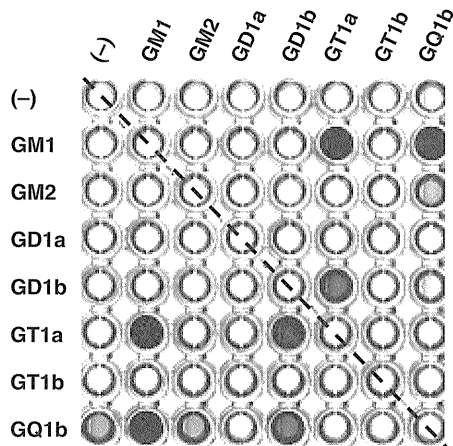
Fig. 1 An ELISA plate showing the binding activities of a serum antibody that recognizes a combination of [Galβ1-3GalNAc] and [NeuAcα2-8NeuAcα2-3 Galβ1-3GalNAc] in the terminal residues. All the wells in each line and column were coated with a respective ganglioside (e.g. the wells in the first line and column were coated only with a single ganglioside, the well in the eighth line and the second column was coated with GQ1b and GM1), except for those on the oblique dotted line that were uncoated control wells. The antibody binds strongly to GQ1b/GM1, GQ1b/GD1b, GT1a/GM1 and GT1a/GD1b but only weakly to GQ1b.

Antibodies to GM1/GalNAc–GD1a complex in pure motor GBS

IgG antibodies against GM1 or those against GalNAc–GD1a are known to closely correlate with acute motor axonal neuropathy (Kaida et al. 2000; Willison and Yuki 2002). We investigated antibody activities against the mixture of GM1 and GalNAc–GD1a (GM1/GalNAc–GD1a complex) in a large population of patients with GBS. The results showed that ten of 224 GBS patients had IgG antibodies to the GM1/GalNAc–GD1a complex (Kaida et al. 2008a).

We then analyzed the clinical and electrophysiologic findings of those 10 anti-GM1/GalNAc–GD1a-positive patients. Respiratory infections preceded the neurological onset in six cases and gastrointestinal infections in two cases. Therefore, although *Campylobacter jejuni* is an infectious agent that frequently causes the antecedent infection of GBS cases with anti-GM1 and anti-GalNAc–GD1a antibodies, *C. jejuni* may not be the major infectious agent inducing anti-GM1/GalNAc–GD1a complex antibodies. Cranial nerve involvement and sensory signs are infrequent. Early motor conduction block at intermediate nerve segments was found in five patients. Generally, the response to therapy was good. According to the criteria established by Hadden et al. (1998), four were categorized as demyelinative and two were axonal. When judged by other criteria (Ho et al. 1995), four were demyelinative and three were axonal.

Table 1 Representative anti-GSCs antibodies in GBS and FS

Antigen	Associated disease	Frequency (%)	Clinical features
GD1a/GD1b	GBS	7	Severe GBS
GD1b/GT1b	GBS	6	Severe GBS
GM1/GalNAc–GD1a	GBS	4	Pure motor GBS AMCBN
GQ1b/GM1 and related GSCs	FS	41	Infrequent sensory dysfunction
	GBS with OP	28	
GQ1b/GD1a and related GSCs	FS	6	
	GBS with OP	19	

GSC, ganglioside complex; GBS, Guillain-Barré syndrome; FS, Fisher syndrome; AMCBN, acute motor conduction block neuropathy; OP, ophthalmoplegia.
GQ1b/GM1 and related GSCs, GQ1b/GM1, GQ1b/GD1b, GT1a/GM1, GT1a/GD1b; GQ1b/GD1a and related GSCs, GQ1b/GD1a, GT1a/GD1a, GQ1b/GT1b, GT1a /GT1b.

The clinical findings of the 10 GBS patients were consistent with a pure motor variant of GBS. Clinical features of anti-GM1/GalNAc–GD1a IgG-positive GBS resemble those of acute motor conduction block neuropathy (AMCBN), in view of preserved sensory function, early conduction block at intermediate nerve segments and good recovery (Capasso et al. 2003). IgG anti-GM1 antibody (and sometimes anti-GalNAc–GD1a antibody) was reported in their sera. However, IgG anti-GM1 or anti-GalNAc–GD1a antibodies are frequently detected in sera of acute motor axonal neuropathy type GBS and conduction block is not common in such cases. Anti-GM1/GalNAc–GD1a antibody is likely to cause early reversible changes on the axolemma and may be more closely associated with AMCBN than the anti-GM1 or anti-GalNAc–GD1a antibody. GM1 and GalNAc–GD1a may form a complex in the axolemma at nodes of Ranvier or paranodes of the motor nerves, and may be a target antigen in pure motor GBS; especially in the form of AMCBN.

Representative anti-GSCs antibodies in GBS and FS are listed in the Table 1.

Antibodies against ganglioside complexes in chronic neuropathies

Nobile-Orazio et al. (2010) investigated serum IgM antibodies to GSCs in such chronic neuropathies as multifocal motor neuropathy, chronic inflammatory demyelinating polyradiculoneuropathy and IgM paraproteinemic neuropathy. As a result, one of 34 chronic inflammatory demyelinating polyradiculoneuropathy patients had IgM antibody activity to GT1b/GM1 and GT1b/GM2, and one of 23 IgM paraproteinemic neuropathy patients had IgM anti-GM2/GD1b activity.

Production of antibodies against ganglioside complexes

In GBS and related disorders subsequent to *C. jejuni* infection, anti-ganglioside antibodies are shown to be induced by the immune reaction against lipo-oligosaccharides (LOS) of pathogens causing antecedent infection (Willison and Yuki 2002; Van Doorn *et al.* 2008). A similar mechanism can be speculated in the production of anti-GSC antibodies. Kuijf *et al.* (2007) recently reported that such anti-GSC antibodies as anti-GM1/GD1a and GQ1b/GD1a cross-reacted to LOS from the autologous *C. jejuni* strain, indirectly demonstrating that the LOS contained GSC-like structures. However, carbohydrate structures expressed in the LOS may not exactly be the combination of the two carbohydrate chains expected from the reactivity of the serum anti-GSC antibodies.

## Inhibition of the reactivity of the anti-ganglioside antibody by another coexistent ganglioside

If the interaction of two gangliosides creates a new epitope with conformational changes, the binding acitivity of the antibody highly specific to one ganglioside may be lessened by the addition of another ganglioside to make an antigen mixture.

We investigated sera from 17 GBS patients who had IgG antibody reactive only with GD1b in routine antibody assay. For those sera, antibody activity against a mixture of GD1b and another ganglioside was examined and compared the activity with that against GD1b alone. The results showed that the addition of GD1a, GT1a, GT1b, GQ1b and GalNAc–GD1a to GD1b caused marked decrease of the binding activity of anti-GD1b antibodies, suggesting that those gangliosides may interact with GD1b to make a novel epitope which cannot be easily recognized by the anti-GD1b antibodies (Kaida *et al.* 2008b).

In addition, the reduction rates of the binding activities caused by the addition of such gangliosides as GD1a, GT1b, GQ1b and GalNAc–GD1a were significantly more in the antibodies from ataxic patients than in those from non-ataxic patients. The addition of another ganglioside may cause conformational change. Therefore, the more specific the antibody is, the more affected its reactivity should be. It therefore suggests that the anti-GD1b IgG antibodies in ataxic patients may be more specific to GD1b than those in patients without ataxia. This may provide further evidence to the association between anti-GD1b antibody and ataxia (Kusunoki *et al.* 1996).

Thus, the antibodies specific to GD1a/GD1b complex are associated with severe GBS (Fig. 2) and those specific to GD1b itself are associated with the development of ataxia (Fig. 3).

A similar inhibitory effect of neighboring gangliosides has recently been reported in the case of anti-GM1 antibodies by
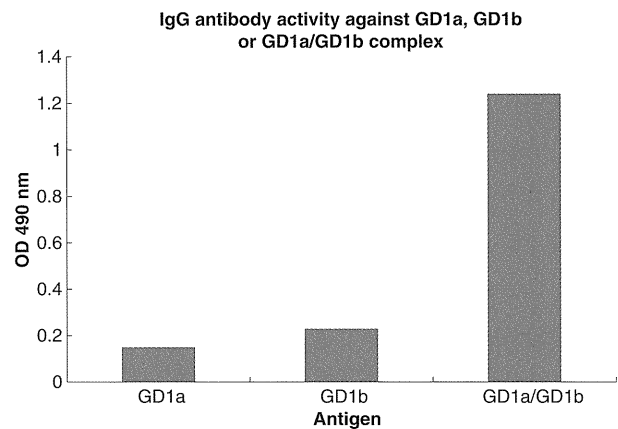
Fig. 2 ELISA result on a serum sample from a patient with severe Guillain-Barré syndrome (Kaida *et al.* 2004). This patient's serum IgG shows strong reaction with a mixture of GD1a and GD1b (GD1a/GD1b) but reacts only weakly with GD1a or GD1b alone.
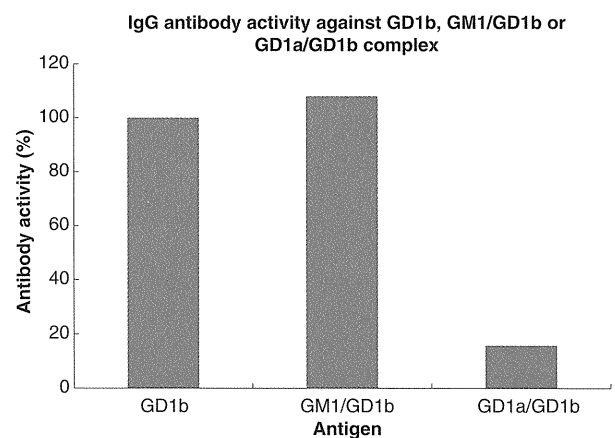
Fig. 3 The IgG antibody activities to mixture antigens in sera from nine GBS patients with ataxia who had only IgG anti-GD1b antibody in routine antibody assay (Kaida *et al.* 2008b). Bars of GM1/GD1b and GD1a/GD1b showed the average activities of the nine patients. Compared with the antibody activity to GD1b alone (100%), the activity was markedly reduced because of the addition of GD1a to GD1b antigen whereas the addition of GM1 did not affect the antibody activity.

Greenshields *et al.* (2009). Negative effects by gangalioside complexes on the binding of IgM anti-GM1 antibodies in sera from patients with chronic immune-mediated neuropathies, particularly multifocal motor neuropathy, have also been reported (Nobile-Orazio *et al.* 2010).

Future studies on the anti-GSC antibodies in the pathogenesis of autoimmune neuropathies

Gangliosides are located in the cell membranes with carbohydrate portions on the outer surfaces, and are preferentially

packaged with cholesterol, forming lipid rafts. Within rafts, gangliosides are considered to interact with important transmembrane receptors or signal transducers (Simons and Ikonen 1997; Hakomori 2002). Anti-GSC antibodies may cause dysfunction of the axon or Schwann cells through their binding to clustered epitopes of glycosphingolipids in the plasma membrane microdomains. Future study on the localization of each ganglioside complex is needed. Animal model of the autoimmune neuropathy mediated by anti-GSC antibodies should also be developed. Such investigations may lead to the understanding of the roles of GSCs in the plasma membrane and of the clinical relevance of the anti-GSCs antibodies.

Acknowledgements

References

Capasso M., Caporale C. M., Pomilio F., Gandolfi P., Lugaresi A. and Uncini A. (2003) Acute motor conduction block neuropathy: another Guillain-Barré syndrome variant. *Neurology* **61**, 617–622.

Chiba A., Kusunoki S., Shimizu T. and Kanazawa I. (1992) Serum IgG antibody to gangalioside GQ1b is a possible marker of Miller Fisher syndrome. *Ann. Neurol.* **31**, 677–679.

Chiba A., Kusunoki S., Otaba H., Machinami R. and Kanazawa I. (1993) Serum anti-GQ1b IgG antibody is associated with ophthalmoplegia in Miller Fisher syndrome and Guillain-Barré syndrome: clinical and immunohistochemical studies. *Neurology* **43**, 1911–1917.

Greenshields K. N., Halstead S. K., Zitman F. M. *et al.* (2009) The neuropathic potential of anti-GM1 autoantibodies is required by the local glycolipid environment in mice. *J. Clin. Invest.* **119**, 595–610.

Hadden R. D. M., Cornblath D. R., Hughes R. A., Zielasek J., Hartung H. P., Toyka K. V. and Swan A. V. (1998) Electrophysiological classification of Guillain-Barré syndrome: clinical associations and outcome: Plasma Exchange/Sandoglobulin Guillain-Barré Syndrome Trial Group. *Ann. Neurol.* **44**, 780–788.

Hakomori S. (2002) The glycosynapse. *Proc. Natl Acad. Sci. USA* **99**, 225–232.

Ho T. W., Mishu B., Li C. Y., Gao C. Y., Cornblath D. R., Griffin J. W., Asbury A. K., Blaser M. J. and McKhann G. M. (1995) Guillain-Barré syndrome in northern China. Relationship to *Campylobacter jejuni* infection and anti-glycolipid antibodies. *Brain* **118**, 597–605.

Kaida K., Kusunoki S., Kamakura K., Motoyoshi K. and Kanazawa I. (2000) Guillain-Barré syndrome with antibody to a ganglioside, *N*-acetylgalactosaminyl GD1a. *Brain* **123**, 116–124.

Kaida K., Morita D., Kanzaki M., Kamakura K., Motoyoshi K., Hirakawa M. and Kusunoki S. (2004) Ganglioside complexes as new target antigens in Guillain-Barré syndrome. *Ann. Neurol.* **56**, 567–571.

Kaida K., Kanzaki M., Morita D., Kamakura K., Motoyoshi K., Hirakawa M. and Kusunoki S. (2006) Anti-ganglioside complex antibodies in Miller Fisher syndrome. *J. Neurol. Neurosurg. Psychiatry* **77**, 1043–1046.

Kaida K., Morita D., Kanzaki M., Kamakura K., Motoyoshi K., Hirakawa M. and Kusunoki S. (2007) Anti-ganglioside complex antibodies associated with severe disability in GBS. *J. Neuroimmunol.* **182**, 212–218.

Kaida K., Sonoo M., Ogawa G., Kamakura K., Ueda-Sada M., Arita M., Motoyoshi K. and Kusunoki S. (2008a) GM1/GalNAc–GD1a complex: a target for pure motor Guillain-Barré syndrome. *Neurology* **71**, 1683–1690.

Kaida K., Kamakura K., Ogawa G., Ueda M., Motoyoshi K., Arita M. and Kusunoki S. (2008b) GD1b-specific antibody induces ataxia in Guillain-Barré syndrome. *Neurology* **71**, 196–201.

Kanzaki M., Kaida K., Ueda M., Morita D., Hirakawa M., Motoyoshi K., Kamakura K. and Kusunoki S. (2008) Ganglioside complexes containing GQ1b as targets in Miller Fisher and Guillain-Barre syndrome. *J. Neurol. Neurosurg. Psychiatry* **79**, 1148–1152.

Kuijf M. L., Godschalk P. C., Gilbert M., Endtz H. P., Tio-Gillen A. P., Ang C. W., van Doorn P. A. and Jacobs B. C. (2007) Origin of ganglioside complex antibodies in Guillain-Barré syndrome. *J. Neuroimmunol.* **188**, 69–73.

Kusunoki S., Shimizu J., Chiba A., Ugawa Y., Hitoshi S. and Kanazawa I. (1996) Experimental sensory neuropathy induced by sensitization with ganglioside GD1b. *Ann. Neurol.* **39**, 424–431.

Kusunoki S., Chiba A. and Kanazawa I. (1999) Anti-GQ1b IgG antibody is associated with ataxia as well as ophthalmoplegia. *Muscle Nerve* **22**, 1071–1074.

Kusunoki S., Kaida K. and Ueda M. (2008) Antibodies against gangliosides and ganglioside complexes in Guillain-Barré syndrome: new aspects of research. *Biochim. Biophys. Acta* **1780**, 441–444.

Liu J.-X., Willison H. J. and Pedrosa-Domellof F. (2009) Immunolocalization of GQ1b and related gangliosides in human extraocular neuromuscular junctions and muscle spindles. *Invest. Ophthalmol. Vis. Sci.* **50**, 3226–3232.

Nobile-Orazio E., Giannotta C. and Briani C. (2010) Anti-ganglioside complex IgM antibodies in multifocal motor neuropathy and chronic immune-mediated neuropathies. *J. Neuroimmunol.* **219**, 119–122.

Ogawa G., Kaida K., Kusunoki S., Ueda M., Kimura F. and Kamakura K. (2009) Antibodies to ganglioside complexes consisting of asialo-GM1 and GQ1b or GT1a in Fisher and Guillain-Barre syndromes. *J. Neuroimmunol.* **214**, 125–127.

Simons K. and Ikonen E. (1997) Functional rafts in cell membranes. *Nature* **387**, 569–572.

Van Doorn P., Ruts L. and Jacobs B. (2008) Clinical features, pathogenesis, and treatment of Guillain-Barré syndrome. *Lancet Neurol.* **7**, 939–950.

Willison H. J. and Yuki N. (2002) Peripheral neuropathies and anti-glycolipid antibodies. *Brain* **125**, 2591–2625.

Interleukin 6 signaling promotes anti-aquaporin 4 autoantibody production from plasmablasts in neuromyelitis optica

Norio Chihara[a,b], Toshimasa Aranami[a,c], Wakiro Sato[a], Yusei Miyazaki[a], Sachiko Miyake[a,c], Tomoko Okamoto[c,d], Masafumi Ogawa[c,d], Tatsushi Toda[b], and Takashi Yamamura[a,c,1]

[a]Department of Immunology, National Institute of Neuroscience, National Center of Neurology and Psychiatry (NCNP), Tokyo 187-8502, Japan; [b]Department of Neurology, Kobe University Graduate School of Medicine, Kobe 650-0017, Japan; and [c]Multiple Sclerosis Center and [d]Department of Neurology, National Center Hospital, NCNP, Tokyo 187-8551, Japan

Neuromyelitis optica (NMO) is an inflammatory disease affecting the optic nerve and spinal cord, in which autoantibodies against aquaporin 4 (AQP4) water channel protein probably play a pathogenic role. Here we show that a B-cell subpopulation, exhibiting the CD19^{int}CD27^{high}CD38^{high}CD180$^-$ phenotype, is selectively increased in the peripheral blood of NMO patients and that anti-AQP4 antibodies (AQP4-Abs) are mainly produced by these cells in the blood of these patients. These B cells showed the morphological as well as the phenotypical characteristics of plasmablasts (PB) and were further expanded during NMO relapse. We also demonstrate that interleukin 6 (IL-6), shown to be increased in NMO, enhanced the survival of PB as well as their AQP4-Ab secretion, whereas the blockade of IL-6 receptor (IL-6R) signaling by anti–IL-6R antibody reduced the survival of PB in vitro. These results indicate that the IL-6–dependent B-cell subpopulation is involved in the pathogenesis of NMO, thereby providing a therapeutic strategy for targeting IL-6R signaling.

neuroinflamatory disease | autoimmunity | multiple sclerosis | central nervous system | IL-6 receptor blockade

Neuromyelitis optica (NMO) is an inflammatory demyelinating disorder characterized by recurrent attacks of severe optic neuritis and myelitis. Unlike the conventional form of multiple sclerosis (CMS), the lesions of NMO tend to spare the cerebral white matter, especially during the early stage (1), and even a single episode of attack can cause serious neurological deficits such as total blindness and paraplegia. Accordingly, accumulation of irreversible damage to the central nervous system (CNS) along with rapid progression of disability is more frequently found in NMO compared with CMS (2).

NMO can be distinguished from CMS by clinical, neuroimaging, and serological criteria (3). It is now known that serum anti-aquaporin 4 (AQP4) autoantibodies can be used as a disease marker of NMO (1, 2). AQP4 is the most abundantly expressed water channel protein in the CNS and is highly expressed in the perimicrovessel astrocyte foot processes, glia limitans, and ependyma (4). Emerging clinical and pathological observations suggest that anti-AQP4 antibodies (AQP4-Abs) play a key role in the pathogenesis of NMO. Prior studies have documented a significant correlation of serum AQP4-Ab levels with the therapeutic efficacy of plasma exchange during clinical exacerbations of NMO (2, 5). In the CNS lesions of NMO, reduced expression of AQP4 on astrocytes is evident even during the early stage (6), which is followed by the occurrence of vasculocentric destruction of astrocytes associated with perivascular deposition of complement and IgG (7).

On the other hand, recent studies have suggested that AQP4-Abs alone are incapable of causing the clinical and pathological features of NMO. In fact, Hinson et al. emphasized the role of cellular immunity in combination with AQP4-Abs by showing that the attack severity of NMO was not correlated with serum AQP4-Ab levels (8). It was also demonstrated that direct injection of IgGs derived from NMO patients into the brains of naïve mice did not cause NMO-like lesions, although brain tissue destruction associated with leukocyte infiltration was elicited by coinjecting human complement (9). Other groups have shown that the passive transfer of IgGs from NMO patients to rats challenged with induction of experimental autoimmune encephalomyelitis (EAE) may cause a decrease in the expression of AQP4 in astrocytes along with worsening of clinical EAE (10–12). In contrast, the transfer of IgGs to unimmunized rats did not cause any pathology. These results suggest that induction of AQP4-Ab–mediated pathology in NMO depends on the presence of complement, leukocytes, and T cells.

Although AQP4-Ab–secreting cells are a potential target for therapy, detailed characteristics of AQP4-Ab–producing cells have not been clarified yet. Because some NMO patients have elevated serum anti-nuclear and anti–SS-A/SS-B Abs (1), as found in patients with systemic lupus erythematosus (SLE) or Sjögren syndrome, NMO might share common pathological mechanisms with these autoimmune diseases. Kikuchi et al. previously reported that CD180$^-$ B cells are activated B cells capable of producing autoantibodies in SLE (13). CD180 is a member of the leucine-rich repeat family of molecules with homology to Toll-like receptor 4 (14), which is highly expressed by naïve and memory B cells but not by plasma cells (15). Odendahl et al. demonstrated that CD27^{high}CD38$^+$ B cells, capable of producing high-affinity IgG (16), are increased in the peripheral blood of SLE patients with some correlation to disease activity (17). Considering the phenotypes of autoantibody-producing cells reported in SLE, we analyzed the expression of CD27, CD38, and CD180 on CD19$^+$ B cells in the peripheral blood of NMO patients. We found that CD27^{high}CD38^{high}CD180$^-$ B cells were significantly increased in AQP4-Ab seropositive patients diagnosed with NMO or NMO spectrum disorder (1) compared with healthy subjects (HS) or CMS patients. Notably, this B-cell subpopulation was found to be a major source of AQP4-Abs in the peripheral blood of AQP4-Ab seropositive patients and depended on interleukin-6 receptor (IL-6R) signaling for survival.

Results

CD27^{high}CD38^{high}CD180^− B Cells Were Increased in the Peripheral Blood of NMO Patients.

Although AQP4-Abs are identified as IgGs (18), no prior study has focused on proportional changes of B-cell subsets in NMO. We therefore performed multicolor flow cytometric analysis of peripheral blood mononuclear cells (PBMC) derived from patients and controls. After starting the study, we soon noticed a remarkable expansion of a distinct B-cell subset in some patients with NMO. The expanded B cells were identified as a population of CD27^{high}, CD38^{high}, and CD180^−, and showed lower expression of CD19 than other B cells (Fig. 1A). Notably, this population did not express the B-cell marker CD20 (Fig. S1). First, we collected samples from patients in remission and analyzed the pooled data. We found that the proportion of this subpopulation among CD19^+ B cells was significantly increased in AQP4-Ab seropositive patients with NMO or NMO spectrum disorder (Fig. 1B) compared with HS or CMS patients. There was no significant difference in the proportion of this B-cell subpopulation between those with typical NMO and those with NMO spectrum disorder. Furthermore, the frequency of this B-cell subpopulation was correlated with the serum AQP4-Ab titer (Fig. S2). Comparison of paired samples obtained from the same patients during relapse and in

remission showed that the CD27^{high}CD38^{high}CD180^− B cells further increased during relapse (Fig. 1C). In contrast, the frequencies of CD27^− naïve B cells (nB) and CD27^+CD38^{−-low} memory B cells (mB) were not altered in AQP4-Ab seropositive patients compared with controls (Fig. S3). The large majority of seropositive patients were treated with corticosteroids. However, the frequency of CD27^{high}CD38^{high}CD180^− cells among CD19^+ B cells was not correlated with the daily corticosteroid dose given to patients (Fig. S4). Moreover, the increase in cells in NMO patients was still evident compared with that in CMS patients similarly treated with corticosteroids (Fig. S5). Taken together, the selective increase in CD27^{high}CD38^{high}CD180^− B cells in seropositive patients was thought to reflect their role in the pathogenesis of NMO but not to be an effect of the corticosteroid treatment.

Expanded Cells Resemble Early Plasma Cells in Gene Expression and Morphology.

To gain insights into the developmental stage of the CD27^{high}CD38^{high}CD180^− B cells, we quantified the mRNA expression of B-cell–associated transcription factors in sorted cell populations. Compared with nB and mB, this population showed much higher expression of B-lymphocyte-induced maturation protein 1 (Blimp-1) and IFN regulatory factor 4 (IRF4), which are essential for the regulation of plasma cell differentiation (19, 20) (Fig. 2A). In contrast, the expression of paired box gene 5 (PAX5), known to be down-regulated in early plasma cell differentiation (21), was reciprocally reduced in the B-cell subset. This gene expression pattern is very similar to that of plasma cells. However, it was notable that the cells of interest expressed CD19, which is not detected in mature plasma cells. Moreover, only 40% of this population expressed the most reliable plasma cell marker CD138 (22). Morphological analysis also confirmed the similarity of this population to plasma cells: they exhibit eccentric nucleus, perinuclear hof region, and abundant cytoplasm. However, they possess a larger nucleus with a lower extent of chromatin clumping compared with CD138^+ plasma cells derived from HS (Fig. 2B). Notably, the CD138^+ population among CD27^{high}CD38^{high}CD180^− cells in NMO patients was
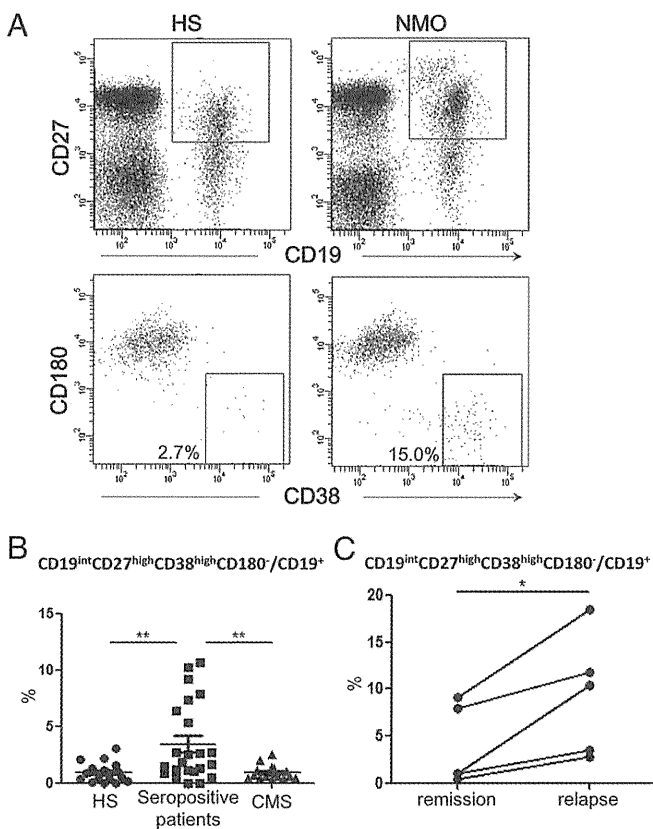
Fig. 1. CD27^{high}CD38^{high}CD180^− B cells increased in NMO patients. (A) A flow cytometric scheme for the analysis of B-cell subpopulations. PBMC from HS and NMO in remission were stained with fluorescence-conjugated anti-CD19, -CD27, -CD38, and -CD180 mAbs. CD19^+CD27^+ cells were partitioned (Upper) and analyzed for expression of CD38 and CD180 (Lower). Values represent the percentage of CD38^{high}CD180^− cells within CD19^+CD27^+ cells. (B) Analysis of the pooled data derived from patients in clinical remission. This shows the percentages of CD27^{high}CD38^{high}CD180^− cells within CD19^+ cells from HS, seropositive patients, and CMS patients (**P < 0.01; Tukey's post hoc test). (C) Comparison of remission and relapse of NMO. Data obtained from the same patients are connected with lines (*P < 0.05; Wilcoxon signed rank test).
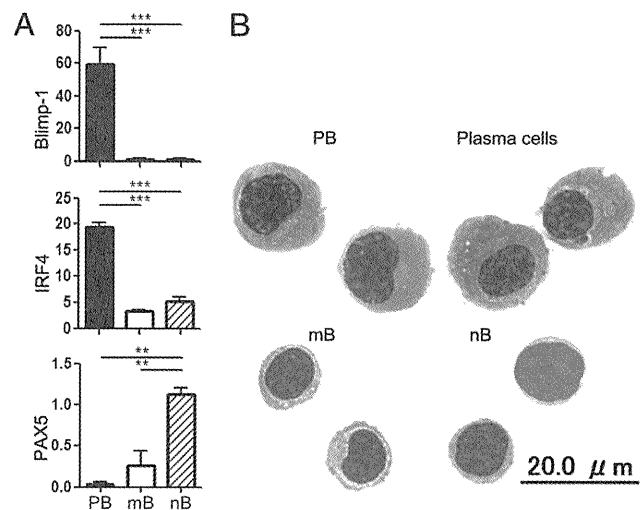
Fig. 2. Resemblance of CD19^{int}CD27^{high}CD38^{high}CD180^− cells to plasma cells. (A) mRNA expression of Blimp-1, IRF4, and PAX5. B-cell subpopulations [CD27^{high}CD38^{high}CD180^− (PB), CD27^− naïve (nB), CD27^+CD38^{−-low} memory (mB)] were sorted by FACS and total RNA was extracted for qRT-PCR analysis. RNA levels were normalized to ACTB for each sample (**P < 0.01; ***P < 0.001; Tukey's post hoc test). (B) May–Grünwald–Giemsa staining of B-cell subpopulations. PB (Upper Left), mB (Lower Left), and nB (Lower Right) from NMO are presented along with morphologically identified plasma cells (CD19^{int}CD27^{high}CD38^{high}CD138^+) from HS (Upper Right).

- 47 -

morphologically indistinguishable from the CD138⁻ population in NMO patients or HS, indicating the immature characteristic of CD27^{high}CD38^{high}CD180⁻ cells (Fig. S6). These phenotypical and morphological characteristics as well as the results of the quantitative real-time PCR (qRT-PCR) analysis indicate that this B-cell population is equivalent to plasmablasts (PB) (22–26). Hereafter, we use the term "PB" to distinguish this population from other B cells.

Expression of B-Cell Cytokine Receptors on PB. Prior studies have identified cytokines that are critically involved in the differentiation and/or survival of plasma cells, including IL-6 and B-cell–activating factor (BAFF). IL-6 induces B-cell differentiation into plasma cells, maintains early plasma cell survival, and enhances plasma cell IgG secretion (24). Besides, IL-6 is elevated in the cerebrospinal fluid (CSF) or peripheral blood of NMO patients compared with that of CMS patients and HS (27, 28). In a rodent autoimmunity model, IL-6 deficiency caused impaired autoantibody secretion by B cells (29). Given the potential role of IL-6 in NMO, we performed flow cytometry analysis for the expression of IL-6R. Results showed remarkable expression of IL-6R on PB, although it was only marginal or absent on mB and nB (Fig. S7). Because BAFF and A proliferation-inducing ligand (APRIL) can also promote the survival of PB (25, 26), we next evaluated the expression of the receptors for BAFF and APRIL, BAFF receptor (BAFF-R), B-cell maturation antigen (BCMA), and transmembrane activator and calcium modulator and cyclophilin ligand interactor (TACI). Expression of BCMA and TACI was selectively up-regulated in PB in parallel with IL-6R. In contrast, BAFF-R was up-regulated in mB and nB, but not in PB (Fig. S7).
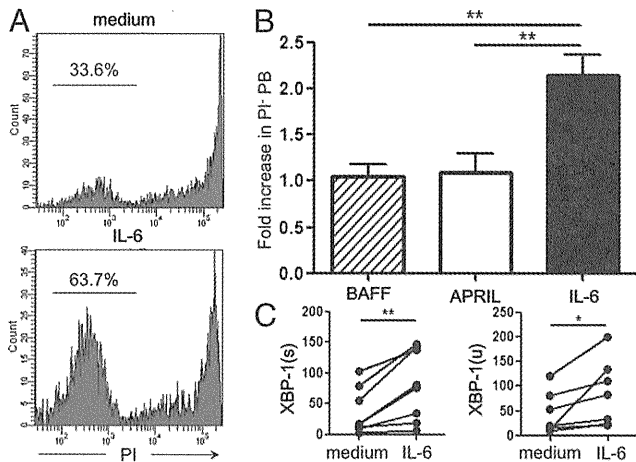
PB Is a Selective Source of AQP4-Abs in Peripheral Blood. We were interested to know whether PB were capable of producing AQP4-Abs upon stimulation with cytokines and, therefore, examined the

ability of IL-6, BAFF, and APRIL to enhance AQP4-Ab secretion by PB. We cultured the isolated PB for 6 d in the presence or absence of each cytokine, and evaluated the presence of AQP4-Abs in the supernatants by measuring IgG binding to Chinese hamster ovary (CHO) cells transfected with the human AQP4 vector (CHO^{AQP4}) or the vector control (CHO^{VC}). We found that IL-6, but not BAFF or APRIL, could significantly enhance AQP4-Ab secretion from PB (Fig. S8), as assessed by specific IgG binding to CHO^{AQP4}. Further study focusing on IL-6 showed that exogenous IL-6 promoted the production of AQP4-specific IgGs from PB (Fig. 3A), but not from the other B-cell subpopulations. Similar results were obtained from six independent experiments (Fig. S9), indicating that PB could be major AQP4-Ab producers in PBMC. In the absence of addition of IL-6, supernatants from PB did not show any significant reactivity to CHO^{AQP4}. To further analyze the AQP4-Ab–secreting potential of each B-cell subpopulation, we next stimulated the cells with a combination of IL-6, IL-21, and anti-CD40 that efficiently induces B-cell differentiation and IgG production (30). This polyclonal stimulation induced the secretion of similar amounts of IgGs from mB and PB. However, only the supernatant of PB specifically reacted to CHO^{AQP4} cell transfectants, indicating that AQP4-Ab–producing B cells were highly enriched in PB (Fig. 3B).

Survival and Functions of PB Depend on IL-6 Signaling. We evaluated the influence of IL-6, BAFF, and APRIL on the survival of PB after 2 d of in vitro culture (Fig. 4A). Among the added cytokines, only IL-6 was found to significantly promote the survival of PB (Fig. 4B). We also assessed the expression levels of X-box-binding protein 1 (XBP-1) in PB by qRT-PCR after 24 h of culture with or without IL-6. XBP-1 is a transcription factor critical for IgG secretion (31), and the splicing process of XBP-1 mRNA yields a more active and stable protein. We found that the expression of both unspliced [XBP-1(u)] and spliced [XBP-1(s)] forms of XBP-1 mRNA was augmented in PB by the ad-
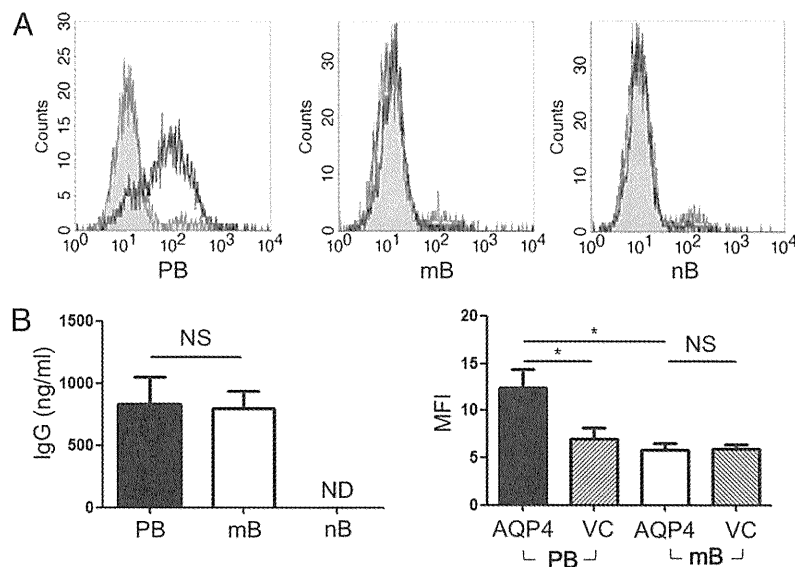
Fig. 3. Production of AQP4-Abs by PB. (A) Using flow cytometry, we examined whether AQP4-Abs could be produced by PB, mB, or nB cells. FACS-sorted cells were cultured with IL-6 (1 ng/mL) for 6 d and supernatants were collected. Supernatant IgGs reactive to CHO^{AQP4} (open histogram) and CHO^{VC} cells (closed histogram) were detected by anti-human IgG secondary antibody. The supernatant from PB (Left), but not from mB or nB, contains IgGs reactive to CHO^{AQP4}, indicating that only PB secrete AQP4-Abs after stimulation with IL-6. (B) Memory B cells (mB) produce IgGs but not AQP4-Abs. B-cell subpopulations were cultured in the presence of IL-6 (1 ng/mL), IL-21 (50 ng/mL), and anti-CD40 mAb (1 μg/mL) for 6 d. IgGs in the culture supernatants were measured by sandwich ELISA (Left) (each assay was performed in quadruplicate). Data from three patients are expressed as mean ± SD. The activity of AQP4-Abs in the culture supernatants from PB and mB was also measured by flow cytometry (Right). Aliquots of CHO^{AQP4} cells (AQP4) and CHO^{VC} cells (VC) (n = 4 for each) were stained with the supernatant of PB or mB from every patient. Data are expressed as median fluorescence intensity values from the results of three patients (*P < 0.05; Tukey's post hoc test). ND, not detected; NS, not significant.

–48–

Fig. 4. medium

A
33.6%
Count
IL-6
63.7%
Count
PI

B
Fold increase in PI⁻ PB
2.5 –
2.0 –
1.5 –
1.0 –
0.5 –
0.0 –
**
**
BAFF   APRIL   IL-6

C
XBP-1(s)
200 –
150 –
100 –
50 –
0 –
**
medium   IL-6

XBP-1(u)
250 –
200 –
150 –
100 –
50 –
0 –
*
medium   IL-6
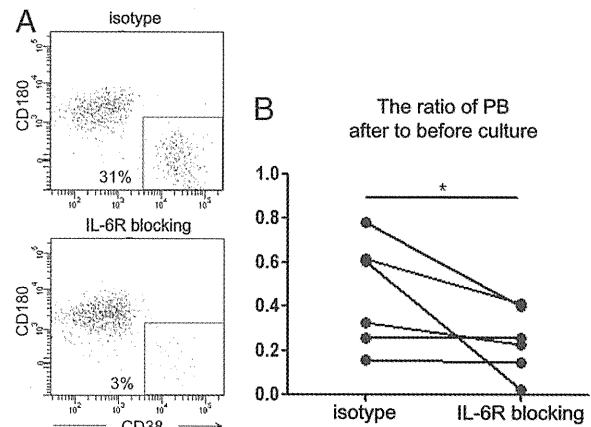
Fig. 4. Effect of exogenous IL-6 on PB. (A) IL-6 promotes the survival of PB. FACS-sorted PB were cultured in the presence or absence of recombinant IL-6 (1 ng/mL) for 2 d. PI staining of cultured PB showed that exogenous IL-6 increased the percentage of surviving cells (Lower) compared with cells cultured in the medium alone (Upper). Values shown are percentages of unstained cells. (B) Comparison of IL-6 with BAFF and APRIL. Here we show that only IL-6 could promote cell survival. Data are expressed as fold increase of % PI⁻ cells following the addition of each cytokine. At least four independent experiments were performed to obtain the results (**$P < 0.01$; Tukey's post hoc test). (C) Effect of IL-6 on XBP-1 expression. FACS-sorted PB were cultured with or without IL-6 for 24 h, and total RNA was extracted from the cells to quantify expression levels of XBP-1(u) and XBP-1(s) by qRT-PCR. Each line connects values obtained from seven independent experiments (*$P < 0.05$; **$P < 0.01$; Wilcoxon signed-rank test).

A
isotype
CD180
31%

IL-6R blocking
CD180
3%
CD38

B
The ratio of PB
after to before culture
1.0 –
0.8 –
0.6 –
0.4 –
0.2 –
0.0 –
*
isotype   IL-6R blocking

Fig. 5. IL-6R blockade selectively inhibits the survival of PB. (A) PBMC were cultured in a medium containing 20% autologous serum in the presence of IL-6R–blocking antibody or its isotype control mAb for 2 d. The cells were stained and analyzed as described in the experiment in Fig. 1A. Data represent the percentages of PB within CD19⁺CD27⁺ cells. A representative pair of six independent experiments is shown. (B) The percentage of PB within CD19⁺ B cells (PB%) was determined for each pair of cultures either with anti–IL-6R mAb (IL-6R–blocking) or isotype control mAb (isotype) before and after starting the culture. Then, the PB survival ratio was calculated for each culture by dividing the PB% at the end of the culture by the PB% obtained before starting the culture. Lines connect the PB survival ratios of six independent experimental pairs to clarify that IL-6R blockade reduces PB survival (*$P < 0.05$; Wilcoxon signed-rank test).

dition of IL-6. These results suggest that IL-6 promoted the survival of PB and enhanced IgG secretion from PB, leading to an increased production of AQP4-Abs in NMO patients (Fig. 4C). In addition, we found that the frequency of PB tended to be increased when serum IL-6 levels were higher than the mean ± 2× SEM of those in HS [PB/PBMC (%) for IL-6 high group 0.62 ± 0.47 (%); PB/PBMC (%) for IL-6 low group 0.15 ± 0.05 (mean ± SD)]. These observations prompted us to address whether the blockade of IL-6R signaling could exhibit any influence on PB. We cultured PBMC derived from AQP4-Ab seropositive patients in the presence of 20% autologous serum and examined the effect of adding anti–IL-6R antibody by counting the number of surviving PB. We found that the frequency of PB among total B cells decreased significantly in the presence of anti–IL-6R mAb (Fig. 5 A and B). Among six patients examined, the PB reduction was remarkable in three patients, but was only marginal in the other patients. Notably, the former group of patients showed higher IL-6 levels in the serum (4.69, 6.47, and 25.5 pg/mL for each patient), compared with the latter (1.42, 1.43, and 2.91 pg/mL). The frequency of other B-cell subpopulations did not change with the addition of anti–IL-6R mAb. These results led us to postulate that in vivo administration of anti–IL-6R mAb may ameliorate NMO.

Discussion

A growing body of evidence suggests that AQP4-Abs play a pathogenic role in NMO (6, 7, 10–12). Here we report that a B-cell subpopulation bearing the CD19^{int}CD27^{high}CD38^{high}CD180⁻ phenotype is responsible for the selective production of AQP4-Abs. The cells that we call PB are vulnerable to IL-6R blockade by anti–IL-6R mAb, leading us to propose anti–IL-6R mAb as a therapeutic option for NMO. Bennett et al. recently reported that plasma cells in CSF are a potential source of pathogenic AQP4-Abs (10). However, this study has not excluded a possible role of AQP4-Abs produced in the peripheral blood. It has been

repeatedly shown that the passive transfer of pathogenic autoantibodies, including AQP4-Abs (10–12, 32), augments the formation of inflammatory lesions in EAE. Therefore, once T-cell–mediated inflammation takes place in the CNS, pathogenic autoantibodies produced outside the CNS are able to enter the CNS compartment. It is also notable that AQP4-Abs are more abundant in the peripheral blood of NMO patients than in their CSF (33). Taken together, we speculate that PB that are expanded in the peripheral blood during relapse may play a critical role in the pathogenesis of NMO by producing AQP4-Abs, although more work is necessary to explore whether PB can enter the CNS.

It is generally thought that circulating IgGs are mainly secreted by long-lived plasma cells residing in healthy bone marrow. It remains unclear how PB secreting AQP4-Abs can differentiate and survive in the peripheral circulation. It has been previously shown that autoantibodies producing plasma cells accumulate in peripheral lymphoid organs (34). It would be interesting to investigate which organs blood PB move to during the course of NMO. The levels of IL-6 in the serum and CSF are elevated in NMO compared with HS or CMS patients (27, 28). In this regard, it is of note that blocking IL-6R signaling was found to dramatically reduce the survival of PB ex vivo, which was dependent on the presence of autologous serum containing IL-6. These results suggest that the increase of PB in AQP4-Ab seropositive patients could be attributed to the increased IL-6 in the serum. We also demonstrated that improved PB survival in the presence of exogenous IL-6 was accompanied by up-regulated expression of XBP-1. It is noteworthy that wild-type and XBP-1⁻/⁻ B cells start to produce more IL-6 after forced overexpression of XBP-1(s), which results in the operation of a positive feedback loop controlling IgG secretion (31). Treatment with anti–IL-6R is promising because IL-6R blockade could terminate this vicious loop that controls the production of autoantibodies.

It has been reported that NMO patients have higher levels of BAFF in the serum or CSF compared with CMS patients (35). BAFF is also known to support plasma cell differentiation and survival of PB induced in vitro (25). However, in our ex vivo

Chihara et al.

– 49 –

study, BAFF did not promote the survival of PB, indicating that PB were not a target for BAFF. We speculate that BAFF might specifically act on an early process of plasma cell differentiation and does not have an influence on cells like PB that have entered a later stage.

IL-6R blockade by humanized mAb against IL-6R (tocilizumab) has proven to be useful for treating immune-mediated diseases, including rheumatoid arthritis (36) and Castleman's disease (37). Here we propose that IL-6R–blocking antibody treatment should be considered as a therapeutic option for NMO. Currently, most NMO patients are being treated with corticosteroids in combination with immunosuppressive drugs and plasma exchange (38). Anti-CD20 mAb, which causes B-cell depletion, has also been used for serious cases of NMO. Because the level of B-cell depletion appears to correlate with the suppressive effects of anti-CD20 in NMO (39), it has been argued that B cells are essential for the pathogenesis of NMO, either via acting as antigen-presenting cells or as autoantibody producers. Weber et al. recently reported that activated antigen-specific B cells serve as antigen-presenting cells and polarize proinflammatory T cells in EAE (40), supporting the view that the therapeutic effects of anti-CD20 might be attributable to the depletion of antigen-presenting B cells. Notably, they also cautioned that elimination of $CD20^+$ cells might deplete nonactivated cells as well as regulatory B cells possessing anti-inflammatory potentials. Although the effect of anti-CD20 on AQP4-Ab–secreting cells has not been reported, it is likely that the majority of PB are not affected because they do not express CD20. Consistent with our prediction, anti-CD20 treatment was not effective in aggressive cases of NMO (41, 42). It appears that selective depletion of activated antigen-specific B cells could be a more promising strategy to improve the efficacy of B-cell–targeted therapies for NMO. In this regard, PB-targeting therapy is a promising approach. Given the efficacy of IL-6R blockade in reducing the number of PB ex vivo, we find it very interesting to explore the effect of anti–IL-6R mAb on NMO.

Materials and Methods

Patients and Controls. A cohort of 24 AQP4-Ab seropositive patients was recruited at the Multiple Sclerosis Clinic of the National Center of Neurology and Psychiatry (NCNP). Among these, 16 met the revised NMO diagnostic criteria (3). The other 8 were diagnosed with NMO spectrum disorder (1) because they did not develop both myelitis and optic neuritis (optic neuritis alone in 6 cases; myelitis alone in 2 cases). Seventeen age- and sex-matched CMS patients and 20 HS were enrolled as controls. Serum AQP4-Ab levels were measured by a previously reported protocol by courtesy of Kazuo Fujihara at Tohoku University (Sendai, Japan) (33). All CMS patients had relapsing-remitting MS and fulfilled McDonald diagnostic criteria (43).

At the time of blood sampling, 21 seropositive patients were receiving corticosteroids (prednisolone 5–25 mg/d). Seven of these patients were also being treated with azathioprine (12.5–100 mg/d) or tacrolimus (3 mg/d). Six CMS patients were receiving low-dose corticosteroids without immunosuppressants. None of the seropositive or CMS patients had received IFN-β, i.v. corticosteroids, plasma exchange, or i.v. immunoglobulins for at least 1 mo before blood sampling. Blood sampling during relapse was performed in six seropositive NMO patients before they received intensive therapy starting with i.v. corticosteroids. Five of these patients were followed up further and blood was collected again after they entered remission. Anti-nuclear and/or anti–SS-A Abs were detected in some of the seropositive patients, but none met the diagnostic criteria for SLE or Sjögren syndrome. Demographic features of the patients are presented in Table 1. The study was approved by the Ethics Committee of the NCNP.

Reagents. The following Abs were used in this study: mAbs against CD38, CD19, CD27, CD20, and PE-streptavidin (Beckman Coulter); mAbs against CD180 and BAFF-R (BD Biosciences); mAbs against IL-6R and TACI as well as Abs against BCMA and CD40 (R&D Systems); rabbit anti-human AQP4 antibody (Santa Cruz Biotechnology); FITC-anti-rabbit IgG (Jackson ImmunoResearch Laboratories); and FITC-anti-human IgG antibody (MP Biomedicals). Recombinant proteins of BAFF (ProSpec), APRIL (Abnova), IL-6 (PeproTech), and IL-21 (Invitrogen) were purchased. Propidium iodide (PI) was obtained from Sigma-Aldrich. RPMI 1640 supplemented with 10% FBS, 2 mM L-glutamine, 100 U/mL penicillin, and 100 mg/mL streptomycin (Life Technologies) was used for cell culture.

Flow Cytometry, Cytology, and Cell Culture. PBMC were separated using density centrifugation on Ficoll-Paque PLUS (GE Healthcare Biosciences). B cells were analyzed and sorted by FACSAria (BD Biosciences). Each B-cell subset was stained with May–Grünwald–Giemsa. To evaluate AQP4-Ab production in vitro, each B-cell subset (1 or 2×10^4) was cultured for 6 d in the medium alone, in the presence of IL-6 (1 ng/mL) or in the presence of IL-6 (1 ng/mL), IL-21 (50 ng/mL), and anti-CD40 (1 μg/mL). Culture supernatants were harvested and analyzed for AQP4-Ab production as described below. To examine the effect of cytokines on the survival of PB, the cells (4×10^3) were cultured in the medium alone or in the presence of BAFF (100 ng/mL), APRIL (300 ng/mL), or IL-6 (1 ng/mL) in 96-well U-bottom plates for 2 d and stained with PI to assess cell survival. In parallel, the cells were cultured for 1 d and harvested to evaluate mRNA expression by qRT-PCR. To assess the effect of IL-6 signaling blockade, PBMC (5×10^5) were preincubated with anti–IL-6R Abs (1 μg/mL) at 4 °C for 20 min, cultured in AIM-V medium (Invitrogen) containing 20% of heat-inactivated serum obtained from each patient in 96-well flat-bottom plates for 2 d, and analyzed by flow cytometry.

Quantitative RT-PCR Analysis. mRNA from each cell subset was isolated according to the manufacturer's instructions using an RNAeasy Kit (Qiagen). RNA was further treated with DNase using the RNase-Free DNase Set (Qiagen) and reverse-transcribed to cDNA using a cDNA synthesis kit (Takara Bio). PCR was performed using iQ SYBR Green Supermix (Takara Bio) on a LightCycler (Roche). RNA levels were normalized to endogenous β-actin (ACTB) for each sample. Primers used are listed in Table S1.

Measurement of Ig Isotypes and Serum IL-6. Secreted IgG in the culture supernatant was quantitated by sandwich ELISA using affinity-purified goat anti-human IgG-Fc (Bethyl Laboratories). Bound IgG was measured according to the manufacturer's instructions. Serum IL-6 was measured by ELISA (R&D Systems) according to the manufacturer's instructions.

AQP4-Ab Detection Assay. Human AQP4-expressing cells were established to detect AQP4-Abs by flow cytometry. A human AQP4 (hAQP4) M23 splice variant from a clone collection (Invitrogen) was amplified by PCR and subcloned into a pIRES-DsRed-Express vector (Clontech). CHO cells (American Type Culture Collection) were transfected with this hAQP4 M23 vector (CHO^{AQP4}) or vector

Table 1. Demographic features

	HS	Seropositive patients	CMS patients
Number	20	24	17
Age	44.7 ± 2.8	47.9 ± 3.2	41.3 ± 3.0
Male:female	5:15	1:23	5:12
Disease duration		12.0 ± 1.6	9.4 ± 2.4
Age of symptom onset		36.1 ± 3.0	31.9 ± 3.4
Relapses in last 2 y		1.4 ± 0.3	0.7 ± 0.2
EDSS score in disease remission		5.0 ± 0.5	2.1 ± 0.6
Other autoantibodies		ANA 13, SS-A 5	ND

Demographic features for HS, AQP4-Ab seropositive patients, and CMS patients. Values are expressed as number or mean ± SEM. ANA, anti-nuclear antibody; ND, not detected; SS-A, anti–SS-A antibody; EDSS, expanded disability status scale.

–50–

control (CHO^{VC}) using FuGENE 6 Transfection Reagent (Roche). After 2 wk of geneticin (Invitrogen) selection, stable clones were established by single-cell sorting. The expression of hAQP4 in the established clones was confirmed using anti-human AQP4 antibody and FITC-anti-rabbit IgG antibody. Reactivity of AQP4-Abs to CHO^{AQP4} was confirmed using seropositive NMO patients' sera diluted at 1:1,000 and FITC-anti-human IgG antibody. To measure the AQP4-Ab activity in culture supernatants, these supernatants were concentrated up to 10 times using an Amicon Ultra 0.5 mL 100K device (Millipore), and 10 μL of the solution was added to 3×10^4 CHO^{AQP4} and CHO^{VC} cells. After incubation on ice for 20 min, cells were washed with sterile PBS containing 1% BSA and stained with FITC-anti-human IgG antibody. After a 10-min incubation on ice, the cells were washed and fixed for 15 min in 2% paraformaldehyde. Then the cells were washed and analyzed by flow cytometry.

Data Analysis. Histogram overlay analysis was performed using Cell Quest software (BD Biosciences). Statistics were calculated using Prism (GraphPad Software). Wilcoxon signed-rank test, Mann–Whitney U test, ANOVA, or Spearman's correlation test were also used when appropriate. Post hoc tests were used as a multiple comparison test after confirmation of equal variances by ANOVA.

1. Wingerchuk DM, Lennon VA, Lucchinetti CF, Pittock SJ, Weinshenker BG (2007) The spectrum of neuromyelitis optica. *Lancet Neurol* 6:805–815.
2. Jarius S, et al. (2008) Mechanisms of disease: Aquaporin-4 antibodies in neuromyelitis optica. *Nat Clin Pract Neurol* 4:202–214.
3. Wingerchuk DM, Lennon VA, Pittock SJ, Lucchinetti CF, Weinshenker BG (2006) Revised diagnostic criteria for neuromyelitis optica. *Neurology* 66:1485–1489.
4. Tait MJ, Saadoun S, Bell BA, Papadopoulos MC (2008) Water movements in the brain: Role of aquaporins. *Trends Neurosci* 31:37–43.
5. Jarius S, et al. (2008) Antibody to aquaporin-4 in the long-term course of neuromyelitis optica. *Brain* 131:3072–3080.
6. Roemer SF, et al. (2007) Pattern-specific loss of aquaporin-4 immunoreactivity distinguishes neuromyelitis optica from multiple sclerosis. *Brain* 130:1194–1205.
7. Misu T, et al. (2007) Loss of aquaporin 4 in lesions of neuromyelitis optica: Distinction from multiple sclerosis. *Brain* 130:1224–1234.
8. Hinson SR, et al. (2009) Prediction of neuromyelitis optica attack severity by quantitation of complement-mediated injury to aquaporin-4-expressing cells. *Arch Neurol* 66:1164–1167.
9. Saadoun S, et al. (2010) Intra-cerebral injection of neuromyelitis optica immunoglobulin G and human complement produces neuromyelitis optica lesions in mice. *Brain* 133:349–361.
10. Bennett JL, et al. (2009) Intrathecal pathogenic anti-aquaporin-4 antibodies in early neuromyelitis optica. *Ann Neurol* 66:617–629.
11. Bradl M, et al. (2009) Neuromyelitis optica: Pathogenicity of patient immunoglobulin in vivo. *Ann Neurol* 66:630–643.
12. Kinoshita M, et al. (2009) Neuromyelitis optica: Passive transfer to rats by human immunoglobulin. *Biochem Biophys Res Commun* 386:623–627.
13. Kikuchi Y, et al. (2002) RP105-lacking B cells from lupus patients are responsible for the production of immunoglobulins and autoantibodies. *Arthritis Rheum* 46:3259–3265.
14. Divanovic S, et al. (2005) Negative regulation of Toll-like receptor 4 signaling by the Toll-like receptor homolog RP105. *Nat Immunol* 6:571–578.
15. Good KL, Avery DT, Tangye SG (2009) Resting human memory B cells are intrinsically programmed for enhanced survival and responsiveness to diverse stimuli compared to naive B cells. *J Immunol* 182:890–901.
16. Wrammert J, et al. (2008) Rapid cloning of high-affinity human monoclonal antibodies against influenza virus. *Nature* 453:667–671.
17. Odendahl M, et al. (2000) Disturbed peripheral B lymphocyte homeostasis in systemic lupus erythematosus. *J Immunol* 165:5970–5979.
18. Hinson SR, et al. (2007) Pathogenic potential of IgG binding to water channel extracellular domain in neuromyelitis optica. *Neurology* 69:2221–2231.
19. Shapiro-Shelef M, et al. (2003) Blimp-1 is required for the formation of immunoglobulin secreting plasma cells and pre-plasma memory B cells. *Immunity* 19:607–620.
20. Klein U, et al. (2006) Transcription factor IRF4 controls plasma cell differentiation and class-switch recombination. *Nat Immunol* 7:773–782.
21. Kallies A, et al. (2007) Initiation of plasma-cell differentiation is independent of the transcription factor Blimp-1. *Immunity* 26:555–566.
22. Jourdan M, et al. (2009) An in vitro model of differentiation of memory B cells into plasmablasts and plasma cells including detailed phenotypic and molecular characterization. *Blood* 114:5173–5181.
23. Manz RA, Hauser AE, Hiepe F, Radbruch A (2005) Maintenance of serum antibody levels. *Annu Rev Immunol* 23:367–386.
24. Kawano MM, Mihara K, Huang N, Tsujimoto T, Kuramoto A (1995) Differentiation of early plasma cells on bone marrow stromal cells requires interleukin-6 for escaping from apoptosis. *Blood* 85:487–494.
25. Avery DT, et al. (2003) BAFF selectively enhances the survival of plasmablasts generated from human memory B cells. *J Clin Invest* 112:286–297.
26. Belnoue E, et al. (2008) APRIL is critical for plasmablast survival in the bone marrow and poorly expressed by early-life bone marrow stromal cells. *Blood* 111:2755–2764.
27. Içöz S, et al. (2010) Enhanced IL-6 production in aquaporin-4 antibody positive neuromyelitis optica patients. *Int J Neurosci* 120:71–75.
28. Yanagawa K, et al. (2009) Pathologic and immunologic profiles of a limited form of neuromyelitis optica with myelitis. *Neurology* 73:1628–1637.
29. Tsantikos E, et al. (2010) Autoimmune disease in Lyn-deficient mice is dependent on an inflammatory environment established by IL-6. *J Immunol* 184:1348–1360.
30. Ettinger R, et al. (2005) IL-21 induces differentiation of human naive and memory B cells into antibody-secreting plasma cells. *J Immunol* 175:7867–7879.
31. Iwakoshi NN, Lee AH, Glimcher LH (2003) The X-box binding protein-1 transcription factor is required for plasma cell differentiation and the unfolded protein response. *Immunol Rev* 194:29–38.
32. Linington C, Bradl M, Lassmann H, Brunner C, Vass K (1988) Augmentation of demyelination in rat acute allergic encephalomyelitis by circulating mouse monoclonal antibodies directed against a myelin/oligodendrocyte glycoprotein. *Am J Pathol* 130:443–454.
33. Takahashi T, et al. (2007) Anti-aquaporin-4 antibody is involved in the pathogenesis of NMO: A study on antibody titre. *Brain* 130:1235–1243.
34. Hoyer BF, et al. (2004) Short-lived plasmablasts and long-lived plasma cells contribute to chronic humoral autoimmunity in NZB/W mice. *J Exp Med* 199:1577–1584.
35. Okada K, Matsushita T, Kira J, Tsuji S (2010) B-cell activating factor of the TNF family is upregulated in neuromyelitis optica. *Neurology* 74:177–178.
36. Nishimoto N, et al. (2004) Treatment of rheumatoid arthritis with humanized anti-interleukin-6 receptor antibody: A multicenter, double-blind, placebo-controlled trial. *Arthritis Rheum* 50:1761–1769.
37. Nishimoto N, et al. (2005) Humanized anti-interleukin-6 receptor antibody treatment of multicentric Castleman disease. *Blood* 106:2627–2632.
38. Okamoto T, et al. (2008) Treatment of neuromyelitis optica: Current debate. *Ther Adv Neurol Disord* 1:5–12.
39. Cree BA, et al. (2005) An open label study of the effects of rituximab in neuromyelitis optica. *Neurology* 64:1270–1272.
40. Weber MS, et al. (2010) B-cell activation influences T-cell polarization and outcome of anti-CD20 B-cell depletion in central nervous system autoimmunity. *Ann Neurol* 68:369–383.
41. Capobianco M, et al. (2007) Variable responses to rituximab treatment in neuromyelitis optica (Devic's disease). *Neurol Sci* 28:209–211.
42. Nasir S, Kerr DA, Birnbaum J (2009) Nineteen episodes of recurrent myelitis in a woman with neuromyelitis optica and systemic lupus erythematosus. *Arch Neurol* 66:1160–1163.
43. Polman CH, et al. (2005) Diagnostic criteria for multiple sclerosis: 2005 revisions to the "McDonald Criteria." *Ann Neurol* 58:840–846.

–51–
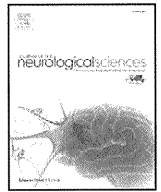
Nationwide survey on the epidemiology of syringomyelia in Japan

Ken Sakushima [a,*], Satoshi Tsuboi [b], Ichiro Yabe [a], Kazutoshi Hida [c], Satoshi Terae [d], Ritei Uehara [b], Imaharu Nakano [e], Hidenao Sasaki [a]

[a] Department of Neurology, Hokkaido University Graduate School of Medicine, Hokkaido, Japan
[b] Department of Public Health, Jichi Medical University, Tochigi, Japan
[c] Department of Neurosurgery, Hokkaido University Graduate School of Medicine, Hokkaido, Japan
[d] Department of Radiology, Hokkaido University Hospital, Hokkaido, Japan
[e] Division of Neurology, Department of Internal Medicine, Jichi Medical University, Tochigi, Japan

ARTICLE INFO

ABSTRACT

Background: Syringomyelia is a rare disease characterized by abnormal fluid-filled cavities within the spinal cord, and is associated with Chiari malformations, arachnoiditis, or spinal cord tumors. The widespread availability of magnetic resonance imaging (MRI) in Japan has allowed for easy identification of syrinxes. The aim of this study was to survey the clinicoepidemiological characteristics of syringomyelia in Japan.
Methods: A 2-stage postal survey was conducted in late 2009. The first survey aimed to estimate the number of patients with syringomyelia, and the second survey aimed to elucidate clinicoepidemiological characteristics. Diagnosis of syringomyelia was based on the findings of MRI or computed tomographic myelography.
Results: In the first survey, we received 2133 responses from 2937 randomly selected departments and collected data of 1215 syringomyelia patients (543 men and 672 women). The total response rate for the first survey was 73%. The estimated prevalence of ambulatory syringomyelia patients in Japan was 1.94 per 100 000. In the second survey, the proportion of asymptomatic syringomyelia patients was 22.7%. Chiari type I malformations and idiopathic syringomyelia were the first and second most common etiologies.
Conclusions: Our nationwide survey indicated that widespread MRI availability has contributed to the diagnosis of both asymptomatic and idiopathic cases.

© 2011 Elsevier B.V. All rights reserved.

1. Introduction

Syringomyelia is a heterogeneous disorder characterized by abnormal fluid-filled cavities or cysts within the spinal cord. The etiologies of syringomyelia can include Chiari malformations, arachnoiditis, trauma, and spinal cord tumors [1–3], but the pathophysiology of syrinx development remains enigmatic. Some cases with Chiari Type I malformations manifested asymptomatic syringomyelia [4]. The reported prevalence was 8.2 to 8.4 per 100 000 in Western countries [5,6]. An epidemiologic survey that collected data from 1243 patients between 1982 and 1991 in Japan showed the predominance of Chiari Type I malformations in syringomyelia, and identified a few cases of spontaneous remission [7]. Surgical treatment for syringomyelia is essential to stop the progression of the disease and further cavity enlargement. However, the previous epidemiologic survey did not

determine the prevalence of the disease in the Japanese population [7].

The diagnosis of syringomyelia has been greatly aided by the development and widespread availability of magnetic resonance imaging (MRI) scanners, which have allowed for the relatively easy identification of syrinxes. Japan has the highest number of magnetic resonance imaging (MRI) scanners per capita, with national healthcare insurance coverage allowing universal access to outpatient hospital care. Hence, both symptomatic and asymptomatic syringomyelia patients can be more adequately examined than was possible prior to MRI facilities becoming widely accessible.

The characteristics of asymptomatic syringomyelia have not been sufficiently investigated. The aim of this study, therefore, was to estimate the prevalence of syringomyelia in Japan and identify its clinicoepidemiological characteristics by taking advantage of the current widespread availability of MRI facilities.

2. Methods

We conducted a 2-stage postal survey according to methods described previously [8,9] in late 2009. The first survey aimed to estimate the number of individuals with syringomyelia, and the second survey aimed to elucidate the clinicoepidemiological characteristics

* Corresponding author at: Department of Neurology, Hokkaido University Graduate School of Medicine, Kita-15, Nishi-7, Kita-ku, Sapporo 060-8638, Japan. Tel.: +81 11 706 6028; fax: +81 11 700 5356.
  E-mail address: sakusima@med.hokudai.ac.jp (K. Sakushima).

of syringomyelia. We collected data from patients diagnosed with syringomyelia by neuroimaging from the departments of neurosurgery, neurology, orthopedics, and pediatrics. We requested the numbers of male and female ambulatory syringomyelia patients from each department in the past year (August 2008 to July 2009).

In the first survey, we adopted a definition of syringomyelia based on neuroimaging: a central or lateralized syrinx detected on MRI (including syrinxes with septums), or a syrinx detected with computed tomographic myelography in patients who could not undergo MRI because of metal in the body. The number of patients with syringomyelia in each institution was counted based on this definition. The departments surveyed were randomly selected by stratified sampling from a list of all hospitals with 20 or more beds; the list was obtained from the Ministry of Health and Welfare. Sampling rates were approximately 5%, 10%, 20%, 40%, 80%, and 100% for the stratum of general hospitals with 20 to 99 beds, 100 to 199 beds, 200 to 299 beds, 300 to 399 beds, 400 to 499 beds, and 500+ beds, respectively. Additionally, all university hospitals in Japan were surveyed.

In the second stage of the survey, we requested details of individual patients from each department that had 1 or more syringomyelia patients. The detailed information for each patient was reported based on a retrospective chart review. Epidemiological items included sex, date of birth, time of onset and diagnosis, family history, symptoms and signs, imaging findings, treatment, and clinical course. Symptoms included motor function, sensory disturbance, autonomic failure, cranial nerve disturbance, and skeletal deformity. Motor functions included weakness, muscle atrophy, spasticity, hypotonus, and planter reflex. Autonomic failure included Horner syndrome, anisocoria, dyshidrosis, abnormal nail development, limb hypertrophy, bladder and rectal disturbance, orthostatic hypotension, impotence, and neurogenic arthropathy.

This study was approved by the Institutional Review Board of Hokkaido University.

2.1. Estimation and statistical analysis

We estimated the prevalence of syringomyelia based on the results from the first stage of the survey. The estimation was based on the assumption that the responses of the departments were independent of the frequency of patients [8,10]. Formulas used to estimate the total number of patients, and the 95% confidence intervals are described below.

The point estimation of prevalence was calculated using the following equation, where SRT_k, RRT_k, NS_k, n_k, N_k, and N_{ki} denote the sampling rate, response rate, the number of sampling departments, the total number of departments, the number of responding departments, and the number of departments with i patients in stratum k, respectively.

$$\hat{\alpha}_k = \frac{1}{SRT_k RRT_k} \sum_i iN_{ki} = \frac{1}{\dfrac{NS_k}{n_k} \dfrac{N_k}{NS_k}} \sum_i iN_{ki} = \frac{n_k}{N_k} \sum_i iN_{ki}.$$

3. Results

In the first survey, we received 2133 responses from 2937 randomly selected departments, and collected data regarding 1215 syringomyelia patients (543 men and 672 women). The total response rate of the first survey was 73%.

Results from the first survey (Table 1) showed that the number of syringomyelia patients who were referred to a hospital between August 2008 and July 2009 was 2475 (95% CI: 2051–2899). The

Table 1
Summary of data collected in the first stage of the survey.

Type s of departments	Type s of hospitals and beds	Total no. of departments	Sampling rate (%)	No. of surveyed departments	No. of departments that responded	Response rate (%)	No. of reported patients	No. of estimated patients
Neurosurgery	General hospitals with ≤99 beds	710	5%	35	22	63%	0	0
	General hospitals with 100–199 beds	528	10%	52	27	52%	7	137
	General hospitals with 200–299 beds	298	20%	59	37	63%	26	209
	General hospitals with 300–399 beds	296	40%	119	73	61%	23	93
	General hospitals with 400–499 beds	167	80%	133	94	71%	40	71
	General hospitals with ≥500 beds	216	100%	216	147	68%	133	195
	University hospitals	113	100%	113	94	83%	267	321
	Subtotal	2328		727	494	68%	496	1027
Neurology	General hospitals with ≤99 beds	506	5%	25	13	52%	0	0
	General hospitals with 100–199 beds	335	10%	34	18	53%	3	56
	General hospitals with 200–299 beds	170	20%	34	27	79%	6	38
	General hospitals with 300–399 beds	170	40%	68	38	56%	7	31
	General hospitals with 400–499 beds	91	100%	91	59	65%	21	32
	General hospitals with ≥500 beds	93	100%	93	60	65%	25	39
	University hospitals	118	100%	118	103	87%	53	61
	Subtotal	1483		463	318	69%	115	257
Orthopedics	General hospitals with ≤99 beds	2278	5%	114	66	58%	4	138
	General hospitals with 100–199 beds	1047	10%	105	70	67%	10	150
	General hospitals with 200–299 beds	436	20%	87	63	72%	10	69
	General hospitals with 300–399 beds	362	40%	145	110	76%	48	158
	General hospitals with 400–499 beds	190	80%	152	107	70%	20	36
	General hospitals with ≥500 beds	228	100%	228	178	78%	120	154
	University hospitals	118	100%	118	98	83%	300	361
	Subtotal	4659		949	692	73%	512	1065
Pediatrics	General hospitals with ≤99 beds	1069	5%	54	32	59%	0	0
	General hospitals with 100–199 beds	613	10%	62	41	66%	0	0
	General hospitals with 200–299 beds	356	20%	71	49	69%	0	0
	General hospitals with 300–399 beds	339	40%	136	105	77%	7	23
	General hospitals with 400–499 beds	184	80%	147	120	82%	11	17
	General hospitals with ≥500 beds	214	100%	214	183	86%	58	68
	University hospitals	114	100%	114	99	87%	16	18
	Subtotal	2889		798	629	79%	92	126
	Total	11359	26%	2937	2133	73%	1215	2475

estimated prevalence of ambulatory syringomyelia patients in Japan was 1.94 per 100 000. In the second survey, we collected reports from 720 of the 1215 patients from the first survey. The response rate for the second survey was 59%. There were 12 duplicated reports, and thus, we integrated the data reported in them.

Results of the second survey (Table 2) described the characteristics of both symptomatic and asymptomatic syringomyelia. The proportion of patients with asymptomatic syringomyelia was 22.7% (161 cases). The mean ages at survey and diagnosis of asymptomatic syringomyelia (28.9 ± 23.3 and 24.4 ± 24.1 years, respectively) were lower than those of patients with symptomatic syringomyelia (40.8 ± 22.8 and 35.3 ± 22.5 years, respectively). Asymptomatic syringomyelia tended to be primarily associated with localized cavities. The proportion of syringomyelia cases with a Chiari type I malformation etiology was higher among symptomatic than asymptomatic syringomyelia patients. Conversely, the proportion of cases with idiopathic etiologies was higher in asymptomatic than in symptomatic syringomyelia.

A subset of patients with symptomatic syringomyelia (Table 3) included both those who had, and those who had not undergone surgical treatment. The mean age at onset and diagnosis of patients who had undergone surgical treatment (29.4 ± 21.0 and 31.6 ± 21.5 years, respectively) was lesser than that of patients who had not received surgical treatment (40.1 ± 22.6 and 44.8 ± 22.3 years, respectively). There were only 2 cases with a family history of the disease. Approximately 11% of patients in each group experienced an improvement in their symptoms. The most common symptom was sensory disturbance, which was reported in 75.3% of patients with surgical treatment and 68.8% of those without surgical treatment. Motor disturbance was the second most common symptom in each

Table 2
Demographics of patients in the second stage of the survey.

	Symptomatic (N = 543)	Asymptomatic (N = 161)	Total (N = 708[a])	Missing
Age at survey (Mean ± SD)	40.8 ± 22.8	28.9 ± 23.3	38.0 ± 23.5	35
Age at diagnosis (mean ± SD)	35.3 ± 22.5	24.4 ± 24.1	32.7 ± 23.4	66
Sex (%)				
Male	41.6	44.1	42.1	1
Female	57.3	53.4	56.5	3
Missing	1.1	2.5	1.4	0
Morphology (%)				
Asymmetry	31.3	8.1	25.8	0
Symmetry	58.9	83.2	64.4	2
Missing	9.8	8.7	9.7	2
Distribution (%)				
Syringobulbia				
Bulbus only	1.5	0.6	1.3	0
Bulbus and spinal cord	5.7	1.2	4.8	1
Syringomyelia				
Cervical cord only	18.6	32.9	21.8	0
Thoracic cord only	7.9	8.7	8.2	1
Lumbosacral cord only	0.9	9.9	3.1	1
Cervical–thoracic	49.4	27.3	44.1	0
Thoracic–lumbosacral	2.6	4.3	3.0	0
Cervical–lumbosacral	4.6	4.3	4.5	0
Missing	8.8	10.6	9.3	1
Etiology (%)				
Chiari type I	53.6	30.4	48.0	0
Chiari type II	4.4	20.5	8.1	0
Bone anomaly	1.1	0.6	1.0	0
Arachnoiditis	5.7	2.5	4.9	0
Trauma	9.6	0.6	7.5	0
Spinal cord tumor	5.2	5.6	5.2	0
Idiopathic	12.9	24.8	15.7	1
Other	6.1	13.0	7.9	2
Suspected two or more	1.1	1.2	1.1	0
Missing	0.4	0.6	0.6	1

[a] Four patients who did not report on the existence of symptoms were excluded.

Table 3
Demographics, clinical history, and manifestations of symptomatic patients.

		Surgical treatment			
		Yes	No	Total	Missing
Number of cases		376	157	543	10
Age at onset (mean ± SD)		29.4 ± 21.0	40.1 ± 22.6	32.3 ± 22.0	
Age at diagnosis (mean ± SD)		31.6 ± 21.5	44.8 ± 22.3	35.3 ± 22.5	
Age at surgery (mean ± SD)		32.6 ± 21.0			
Family history (%)	Yes	0.3	0.6	0.4	0
	No	64.4	59.9	62.2	2
	Unknown/missing	31.1	35.0	32.4	
Course of symptoms after initial diagnosis (%)					
Worsen		51.1	22.3	42.2	2
Unchanged		26.3	56.7	35.5	5
Improved		11.2	10.8	10.9	0
Stop after progression		4.8	5.7	5.0	0
Missing		6.6	4.5	6.4	
Symptoms (%)					
Motor	Yes	59.8	51.0	57.5	7
	No	37.8	45.9	39.4	0
	Unknown/missing	2.4	3.2	3.1	
Sensory	Yes	75.3	68.8	72.7	4
	No	19.9	21.0	19.9	0
	Unknown/missing	4.8	10.2	7.4	
Autonomic	Yes	20.7	19.1	19.9	0
	No	65.2	65.6	64.6	3
	Unknown/Missing	14.1	15.3	15.5	
Cranial nerves	Yes	10.1	7.0	9.2	1
	No	83.2	80.9	81.4	2
	Unknown/missing	6.6	12.1	9.4	
Skeletal deformity	Yes	31.4	22.9	29.3	5
	No	64.9	75.2	67.4	4
	Missing	3.7	1.9	3.3	
Past history (%)					
CNS infections	Yes	3.5	3.8	3.7	1
	No	80.6	74.5	78.3	5
	Unknown/missing	16.0	21.7	18.0	4
Injuries of head or spine	Yes	11.4	10.2	10.9	0
	No	76.3	75.8	75.7	5
	Unknown/missing	12.2	14.0	13.4	
Surgery of head or spine	Yes	13.8	12.1	13.4	2
	No	77.4	77.7	77.0	5
	Unknown/missing	8.8	10.2	9.6	
Problems at delivery	Yes	2.1	1.3	2.0	1
	No	66.2	59.9	63.9	4
	Unknown/missing	31.6	38.9	34.1	

group (59.8% and 51.0%, respectively). Patient histories showed that approximately one-tenth of the patients in each group had previous injuries of the head or spine.

The characteristics of patients in each age group (Table 4) showed that the prevalence of idiopathic syringomyelia was higher in adults, particularly in the elderly, than in children.

Fig. 1 shows the distributions of patient's ages at the time of survey (Fig. 1A), age at diagnosis (Fig. 1B), age at surgical treatment (Fig. 1C), and year of diagnosis (Fig. 1D). The distribution of ages at survey consisted of 2 peaks, at 10 to 20 years of age, and at 60 to 70 years of age. The distribution of age at diagnosis showed a higher proportion of 0- to 20-year-olds. Finally, the distribution of diagnosis year showed an acute increment in the number of cases diagnosed in more recent years.

4. Discussion

This study revealed the prevalence (1.94 per 100 000) and characteristics of ambulatory syringomyelia patients in Japan. Among these patients, the prevalence of asymptomatic syringomyelia was 22.6%,